

and facile skin markings are one solution to this problem. This author conducted a multicenter prospective study on the effectiveness of pre-operative breast CT imaging in surgical planning for patients undergoing BCS [23]. The surgeons marked the line of planned excision on the skin based on information from palpation, MMG, and US before CT, which was also recorded on the CT image. Contrast-enhanced breast CT was performed in the supine surgical position. The CT results were used to help determine the

extent of resection. The surgeons widened the extent of resection in 42 (14.1%; 95% confidence interval 10.1–18.1%) out of a total of 297 patients based on the CT findings. Breast CT correctly modified the extent of surgery in 13.1% and overexcision in 1%. An example of a correctly modified case using CT is shown in Fig. 2. CT was especially effective in cases of invasive lobular carcinoma and apocrine carcinoma. The efforts taken to simulate the patient's positioning that was subsequently used in the

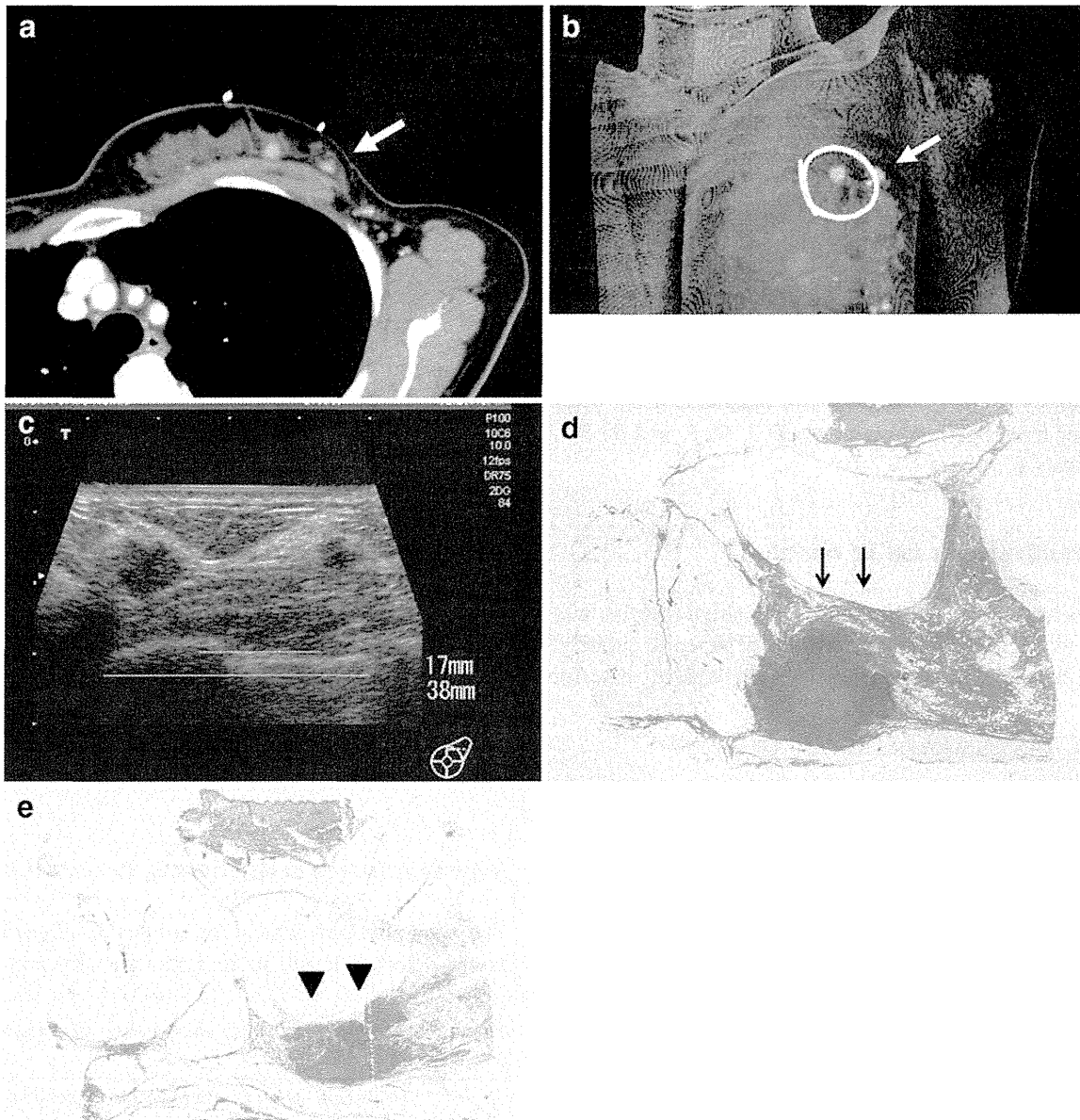


Fig. 2 An instance in which CT successfully affected surgical management. **a** CT image showing an enhancing lesion (*arrow*) lateral to the main tumor which suggested that it was located outside the planned resection line. The angiocatheter can be seen on the skin demarcating the pre CT planned resection line. **b** Maximum intensity projection image of the right breast. The *white line* indicates the surgical line that was originally planned. **c** Second look

ultrasonography revealed a second tumor with an 8 mm diameter located 17 mm lateral to the main tumor. We modified the resection line to widen the lateral side. **d** Surgical specimen (H&E). The *arrows* indicate the main tumor which was an invasive ductal carcinoma. **e** The *triangles* indicate the second tumor which was an invasive ductal carcinoma located in the modified excised specimen

operating room, and surgical marking, brought about this excellent result.

Harada-Shoji et al. [24] reported excellent incidence of negative margins after BCS using a dedicated skin marker. Seven lines marked on the patient's skin using an oil-based paint enabled accurate resection with incidence of positive margins of 2.2%. These markings were effective when they were scanned with the patient in the supine position, which is the position used during surgery. Second-look US with the patient in the supine position in order to utilize the information obtained when the patient was in the prone position during MRI is widespread. Real time virtual sonography in the supine position has been reported to be useful for identifying enhancing breast lesions originally detected by MRI [25].

Limitations

The disadvantage of CT is radiation exposure. Some studies have compared the accuracy of MD-CT and MRI in evaluation of the intraductal spread of breast cancer. CT has been shown to be inferior in sensitivity to MRI and superior [26, 27] or equivalent [28] in specificity. The low-grade intraductal component and lobular carcinoma in situ tended not to be depicted as accurately using CT as the high-grade intraductal component [11]. Mucinous carcinoma was weakly enhanced by the contrast medium, and as a consequence tumor extent was sometimes underestimated [26].

In conclusion, CT carried out with the patient in the supine position, accompanied with adequate marking, is effective for preoperative determination of the optimum extent of breast cancer surgery.

References

- Kang DK, Kim MJ, Jung YS, Yim H. Clinical application of multidetector row computed tomography in patient with breast cancer. *J Comput Assist Tomogr.* 2008;32(4):583–98.
- Inoue M, Sano T, Watai R, Ashikaga R, Ueda K, Watatani M, et al. Dynamic multidetector CT of breast tumors: diagnostic features and comparison with conventional techniques. *AJR Am J Roentgenol.* 2003;181(3):679–86.
- Porter G, Steel J, Paisley K, Watkins R, Holgate C. Incidental breast masses detected by computed tomography: are any imaging features predictive of malignancy? *Clin Radiol.* 2009;64(5):529–33.
- Moyle P, Sonoda L, Britton P, Sinnatamby R. Incidental breast lesions detected on CT: what is their significance? *Br J Radiol.* 2010;83(987):233–40.
- Kim SM, Park JM. Computed tomography of the breast. Abnormal findings with mammographic and sonographic correlation. *J Comput Assist Tomogr.* 2003;27(5):761–70.
- Miyake K, Hayakawa K, Nishino M, Nakamura Y, Morimoto T, Urata Y, et al. Benign or malignant? Differentiating breast lesions with computed tomography attenuation values on dynamic computed tomography mammography. *J Comput Assist Tomogr.* 2005;29(6):772–9.
- Prionas ND, Lindfors KK, Ray S, Huang SY, Beckett LA, Monsky WL, et al. Contrast enhanced dedicated breast CT: initial clinical experience. *Radiology.* 2010;256(3):714–23.
- Perrone A, Lo Mele L, Sassi S, Marini M, Testaverde L, Izzo L. MDCT of the breast. *AJR Am J Roentgenol.* 2008;190(6):1644–51.
- Kuroki Suzuki S, Kuroki Y, Ishikawa T, Takeo H, Moriyama N. Diagnosis of breast cancer with multidetector computed tomography: analysis of optimal delay time after contrast media injection. *Clin Imaging.* 2010;34(1):14–9.
- Nakano S, Sakamoto H, Ohtsuka M, Mibu A, Karikomi M, Sakata H, et al. Successful use of multi detector row computed tomography for detecting contralateral breast cancer. *J Comput Assist Tomogr.* 2011;35(1):148–52.
- Akashi Tanaka S, Fukutomi T, Miyakawa K, Uchiyama N, Tsuda H. Diagnostic value of contrast enhanced computed tomography for diagnosing the intraductal component of breast cancer. *Breast Cancer Res Treat.* 1998;49:79–86.
- Akashi Tanaka S, Fukutomi T, Sato N, Miyakawa K. The role of computed tomography in the selection of breast cancer treatment. *Breast Cancer.* 2003;10(3):198–203.
- Takase K, Furuta A, Harada N, Takahashi T, Igarashi K, Chiba Y, et al. Assessing the extent of breast cancer using multidetector row helical computed tomography. *J Comput Assist Tomogr.* 2006;30(3):479–85.
- Fujita T, Doihara H, Takabatake D, Takahashi H, Yoshitomi S, Ishibe Y, et al. Multidetector row computed tomography for diagnosing intraductal extension of breast carcinoma. *J Surg Oncol.* 2005;91(1):10–6.
- Doihara H, Fujita T, Takabatake D, Takahashi H, Ogasawara Y, Shimizu N, et al. Clinical significance of multidetector row computed tomography in breast surgery. *Breast J.* 2006;12(5 Suppl 2):S204–9.
- Inoue T, Tamaki Y, Hamada S, Yamamoto S, Sato Y, Tamura S, et al. Usefulness of three dimensional multidetector row CT images for preoperative evaluation of tumor extension in primary breast cancer patients. *Breast Cancer Res Treat.* 2005;89(2):119–25.
- Uematsu T, Sano M, Homma K, Shiina M, Kobayashi S. Three dimensional helical CT of the breast: accuracy for measuring extent of breast cancer candidates for breast conserving surgery. *Breast Cancer Res Treat.* 2001;65(3):249–57.
- Shien T, Akashi Tanaka S, Yoshida M, Hojo T, Iwamoto E, Miyagawa K, et al. Usefulness of preoperative multidetector row computed tomography in evaluating the extent of invasive lobular carcinoma in patients with or without neoadjuvant chemotherapy. *Breast Cancer.* 2009;16(1):30–6.
- Taira N, Ohsumi S, Takabatake D, Hara F, Takashima S, Aogi K, et al. Contrast enhanced CT evaluation of clinically and mammographically occult multiple breast tumors in women with unilateral early breast cancer. *Jpn J Clin Oncol.* 2008;38(6):419–25.
- Bleicher RJ, Ciocca RM, Egleston BL, Sesa L, Evers K, Sigurdson ER, et al. Association of routine pretreatment magnetic resonance imaging with time to surgery, mastectomy rate, and margin status. *J Am Coll Surg.* 2009;209(2):180–7.
- Turnbull L, Brown S, Harvey I, Olivier C, Drew P, Napp V, et al. Comparative effectiveness of MRI in breast cancer (COMICE) trial: a randomised controlled trial. *Lancet.* 2010;375(9714):563–71.
- Peters NH, van Esser S, van den Bosch MA, Storm RK, Plaisier PW, van Dalen T, et al. Preoperative MRI and surgical management in patients with nonpalpable breast cancer: the

- MONET randomised controlled trial. *Eur J Cancer*. 2011;47(6): 879–86.
23. Akashi Tanaka S. Evaluation of the usefulness of breast CT imaging in delineating tumor extent and guiding surgical management: a prospective multi institutional study. *Ann Surg*. (in press).
 24. Harada Shoji N, Yamada T, Ishida T, Amari M, Suzuki A, Moriya T, et al. Usefulness of lesion image mapping with multidetector row helical computed tomography using a dedicated skin marker in breast conserving surgery. *Eur Radiol*. 2009; 19(4):868–74.
 25. Nakano S, Yoshida M, Fujii K, Yorozya K, Mouri Y, Kousaka J, et al. Fusion of MRI and sonography image for breast cancer evaluation using real time virtual sonography with magnetic navigation: first experience. Preoperative MRI marking technique for the planning of breast conserving surgery. *Jpn J Clin Oncol*. 2009;39(9):552–9.
 26. Uematsu T, Yuen S, Kasami M, Uchida Y. Comparison of magnetic resonance imaging, multidetector row computed tomography, ultrasonography, and mammography for tumor extension of breast cancer. *Breast Cancer Res Treat*. 2008;112(3): 461–74.
 27. Nakahara H, Namba K, Wakamatsu H, Watanabe R, Furusawa H, Shirouzu M, et al. Extension of breast cancer: comparison of CT and MRI. *Radiat Med*. 2002;20(1):17–23.
 28. Shimauchi A, Yamada T, Sato A, Takase K, Usami S, Ishida T, et al. Comparison of MDCT and MRI for evaluating the intraductal component of breast cancer. *Am J Roentgenol*. 2006; 187(2):322–9.

Analysis of Ki-67 Expression With Neoadjuvant Anastrozole or Tamoxifen in Patients Receiving Goserelin for Premenopausal Breast Cancer

Hiroji Iwata, MD¹; Norikazu Masuda, MD²; Yasuaki Sagara, MD³; Takayuki Kinoshita, MD⁴;
Seigo Nakamura, MD⁵; Yasuhiro Yanagita, MD⁶; Reiki Nishimura, MD⁷; Hiroataka Iwase, MD⁸; Shunji Kamigaki, MD⁹;
Hiroyuki Takei, MD¹⁰; Hitoshi Tsuda, MD¹¹; Nobuya Hayashi, BA¹²; and Shinzaburo Noguchi, MD¹³

BACKGROUND: The increasing costs associated with large-scale adjuvant trials mean that the prognostic value of biologic markers is increasingly important. The expression of nuclear antigen Ki-67, a marker of cell proliferation, has been correlated with treatment efficacy and is being investigated for its value as a predictive marker of therapeutic response. In the current study, the authors explored correlations between Ki-67 expression and tumor response, estrogen receptor (ER) status, progesterone receptor (PgR) status, and histopathologic response from the STAGE study (Study of Tamoxifen or Arimidex, combined with Goserelin acetate to compare Efficacy and safety). **METHODS:** In a phase 3, double-blind, randomized trial (National Clinical Trials identifier NCT00605267), premenopausal women with ER-positive, early stage breast cancer received either anastrozole plus goserelin or tamoxifen plus goserelin for 24 weeks before surgery. The Ki-67 index, hormone receptor (ER and PgR) status, and histopathologic responses were determined from histopathologic samples that were obtained from core-needle biopsies at baseline and at surgery. Tumor response was determined by using magnetic resonance imaging or computed tomography. **RESULTS:** In total, 197 patients were randomized to receive either anastrozole plus goserelin ($n = 98$) or tamoxifen plus goserelin ($n = 99$). The best overall tumor response was better for the anastrozole group compared with the tamoxifen group both among patients who had a baseline Ki-67 index $\geq 20\%$ and among those who had a baseline Ki-67 index $< 20\%$. There was no apparent correlation between baseline ER status and the Ki-67 index in either group. Positive PgR status was reduced from baseline to week 24 in the anastrozole group. **CONCLUSIONS:** In premenopausal women with ER-positive breast cancer, anastrozole produced a greater best overall tumor response compared with tamoxifen regardless of the baseline Ki-67 index. *Cancer* 2013;119:704-13. © 2012 American Cancer Society.

KEYWORDS: anastrozole, aromatase inhibitor, biomarker, neoadjuvant, Ki-67, premenopausal breast cancer.

INTRODUCTION

In addition to ablative surgery, radiotherapy, and cytotoxic chemotherapy, an additional standard treatment option for premenopausal women with estrogen receptor (ER)-positive breast cancer is the ER antagonist tamoxifen, either alone or in combination with ovarian function suppression.¹ Temporary and potentially reversible ovarian suppression can be achieved by treatment with a luteinizing hormone-releasing hormone analog, such as goserelin. Goserelin in combination with tamoxifen has demonstrated improved progression-free survival and disease-free survival compared with goserelin alone in premenopausal women with hormone receptor-positive (ER-positive and/or progesterone receptor [PgR]-positive) breast cancer in the advanced² and adjuvant³ settings.

Nonsteroidal aromatase inhibitors (AIs), including anastrozole and letrozole, and the irreversible steroidal aromatase inactivator exemestane have demonstrated improved efficacy compared with tamoxifen in the advanced⁴⁻⁷ and adjuvant⁸⁻

Corresponding author: Shinzaburo Noguchi, MD, Department of Breast and Endocrine Surgery, Osaka University Graduate School of Medicine, 2-15 Yamadaoka Suita City, Osaka 565-0871, Japan; Fax: (011) 81-6-6789-3779; noguchi@onsurg.med.osaka-u.ac.jp

¹Department of Breast Oncology, Aichi Cancer Center Hospital, Aichi, Japan; ²Department of Surgery, Breast oncology, National Hospital Organization, Osaka National Hospital, Osaka, Japan; ³Department of Breast Surgery, Sagara Hospital, Kagoshima, Japan; ⁴Division of Breast Surgery, National Cancer Center Hospital, Tokyo, Japan; ⁵Department of Breast Surgical Oncology, St. Luke's International Hospital, Tokyo, Japan; ⁶Department of Breast Oncology, Gunma Cancer Center, Gunma, Japan; ⁷Department of Breast and Endocrine Surgery, Kumamoto City Hospital, Kumamoto, Japan; ⁸Department of Breast and Endocrine Surgery, Kumamoto University Hospital, Kumamoto, Japan; ⁹Department of Surgery, Sakai Municipal Hospital, Osaka, Japan; ¹⁰Department of Breast Surgery, Saitama Cancer Center, Saitama, Japan; ¹¹Department of Pathology and Clinical Laboratories, National Cancer Center Hospital, Tokyo, Japan; ¹²Department of Research and Development, AstraZeneca, Osaka, Japan; ¹³Department of Breast and Endocrine Surgery, Osaka University Graduate School of Medicine, Osaka, Japan

Seigo Nakamura's current address: Department of Breast Surgical Oncology, Showa University Hospital, Tokyo, Japan.

Presented as an oral presentation at the 47th Annual Meeting of the American Society of Clinical Oncology; June 3-7, 2011; Chicago, IL.

We thank Takayuki Kobayashi, Harumi Nakamura, Masafumi Kurosumi, and Futoshi Akiyama for their roles as members of the Central Pathological Review Committee. We also thank Simon Vass, PhD, from Complete Medical Communications, who provided medical writing support that was funded by AstraZeneca.

DOI: 10.1002/cncr.27818, **Received:** May 18, 2012; **Revised:** August 9, 2012; **Accepted:** August 13, 2012, **Published online** September 12, 2012 in Wiley Online Library (wileyonlinelibrary.com)

¹² treatment settings. Therefore, AIs in combination with ovarian suppression have been evaluated for the treatment of premenopausal women with ER-positive breast cancer.^{13,14}

Neoadjuvant treatment for breast cancer provides an opportunity for downstaging of large tumors to allow patients to undergo breast-conserving surgery rather than mastectomy. Chemotherapy can offer an effective neoadjuvant treatment; however, increasing evidence suggests that ER-positive tumors are less sensitive to chemotherapy.¹⁵ It has been demonstrated that neoadjuvant endocrine therapy has efficacy in the treatment of ER-positive disease among postmenopausal women, resulting in similar objective response rates and rates of breast-conserving surgery for AIs compared with more cytotoxic chemotherapy.¹⁶ Therefore, the role of neoadjuvant endocrine therapy in premenopausal women is also of interest.

With the increasing costs associated with large-scale adjuvant trials, both the prognostic value of biologic markers and the long-term predictive value of short-term trials are increasingly important. The expression of nuclear antigen Ki-67, a marker of cell proliferation, reportedly has been correlated with treatment efficacy and is being investigated for its value as a predictive marker of therapeutic response.¹⁷ In a cross-trial comparison, an increased reduction in Ki-67 expression after neoadjuvant treatment with anastrozole compared with tamoxifen was observed consistently; and increased progression-free survival has been reported for anastrozole versus tamoxifen in the adjuvant Arimidex, Tamoxifen, Alone or in Combination (ATAC) trial.^{8,18,19}

The STAGE study (Study of Tamoxifen or Arimidex Combined With Goserelin Acetate to Compare Efficacy and Safety) was the first randomized trial to compare anastrozole plus goserelin versus tamoxifen plus goserelin in the neoadjuvant setting (24 weeks of therapy) in premenopausal women with ER-positive and human epidermal growth factor receptor 2 (HER2)-negative, operable breast cancer. The patients who received anastrozole plus goserelin in that trial had a superior best overall tumor response compared with the patients who received tamoxifen plus goserelin, as measured on magnetic resonance imaging (MRI) or computed tomography (CT) studies (anastrozole plus goserelin, 64.3%; tamoxifen plus goserelin, 37.4%; estimated difference, 26.9%; 95% confidence interval [CI], 13.5-40.4; $P < .001$). The treatment effect was consistently in favor of anastrozole, regardless of the measurement methods (caliper and ultrasound). The histopathologic response rate also was better in the anastrozole group (anastrozole plus goserelin, 41.8%; tamoxifen plus goserelin, 27.3%; estimated difference, 14.6%; 95%

CI, 1.4-27.7; $P = .032$). Both treatment regimens were well tolerated, consistent with the known safety profiles of anastrozole, tamoxifen, and goserelin.²⁰ The geometric mean Ki-67 index at baseline was 21.9% in the anastrozole group and 21.6% in the tamoxifen group. At week 24, the Ki-67 index was reduced in both treatment groups (to 2.9% in the anastrozole group and to 8% in the tamoxifen group). The reduction from baseline to week 24 was significantly greater with anastrozole than with tamoxifen. The estimated ratio of reduction between groups was 0.35 (95% CI, 0.24-0.51; $P < .001$).²⁰ Here, we report an exploratory analysis of the STAGE study that investigated potential correlations between the Ki-67 index and the best overall tumor response, ER status, PgR status, or histopathologic response.

MATERIALS AND METHODS

Study Design and Patients

In this phase 3, double-blind, randomized, parallel-group, multicenter trial, the participating patients were premenopausal women ≥ 20 years with ER-positive and HER2-negative breast cancer who had operable and measurable lesions (tumors measuring 2-5 cm, negative lymph node status [N0], and no metastases [M0]). Inclusion and exclusion criteria have been described previously.²⁰

Patients were randomized 1:1 to receive either oral anastrozole 1 mg daily with a tamoxifen placebo or oral tamoxifen 20 mg daily with an anastrozole placebo. Both treatment groups received goserelin 3.6 mg as a subcutaneous injection every 28 days. Treatment continued for 24 weeks before surgery or until patients met any criterion for discontinuation.

The primary study endpoint was the best overall tumor response during the 24-week neoadjuvant treatment period. Secondary endpoints included histopathologic response, changes in estrone (E_1) and estradiol (E_2) serum and breast tumor tissue concentrations, changes in Ki-67 expression, and tolerability. For this exploratory analysis, we assessed correlations between Ki-67 expression and tumor response, ER status, PgR status, or histopathologic response.

The protocol was approved by an institutional review board at all study sites, and all enrolled patients provided written informed consent. The study (National Clinical Trials identifier NCT00605267) was conducted in accordance with the Declaration of Helsinki and good clinical practice, the applicable local regulatory requirements, and the AstraZeneca policy on Bioethics.

Assessments

Tumor measurements were performed using caliper measurements, ultrasound, or MRI or CT studies. The

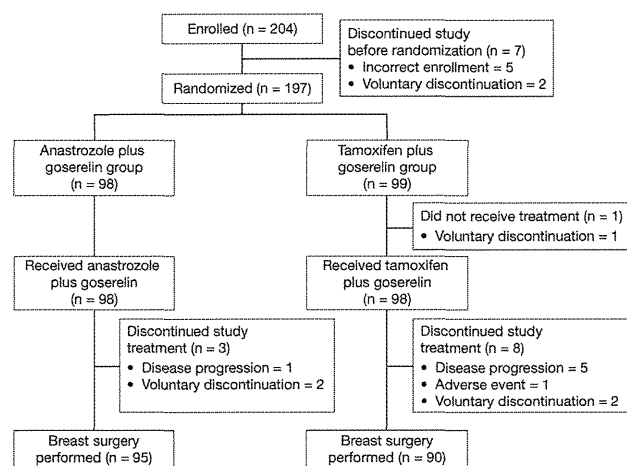


Figure 1. This is a CONSORT (Consolidated Standards of Reporting Trials) diagram of the current study.

primary analysis indicated that the best overall tumor response for anastrozole versus tamoxifen was consistent, regardless of the measurement method used.²⁰ We present tumor response data from the MRI or CT measurements at day 0 and at 24 weeks. The objective tumor response was assessed according to modified Response Evaluation Criteria in Solid Tumors (RECIST).²¹

The status of Ki-67, ER, and PgR was determined using histopathologic core-needle biopsy specimens that were collected at baseline and at surgery. Tissue sections were fixed in formalin and stored at room temperature before immunohistochemical staining. Ki-67 expression was determined by staining sections with an anti-MIB-1 antibody at a central laboratory (SRL Inc., Tokyo, Japan) for assessment by a central review board. For all slides, photomicrographs were taken from 3 to 5 hotspots at $\times 20$ magnification using light microscopy. Two pathologists independently assessed the photomicrographs, and the Ki-67 index was calculated as the ratio of Ki-67-positive cancer cells from a total of 1000 cancer cells. ER-positive status and PgR-positive status at baseline were defined as $\geq 10\%$ staining of cancer cell nuclei determined by a pathologist at each individual study site (nuclei were assessed using mouse monoclonal antibody clones 6F11 and 16, respectively). Staining for ER and PgR also was assessed in parallel using Allred scores by the Central Pathologist Review Committee.²² An Allred score (the proportion score plus the intensity score) of ≥ 3 defined ER or PgR positivity, a score from ≥ 3 to < 7 indicated medium expression, and a score of ≥ 7 indicated rich expression.

Histopathologic effects were assessed by comparing histopathologic samples that were obtained at baseline and at surgery. For the assessment of histopathologic

response, the following categories were used: grade 0 indicated no response; grade 1a, marked change in < 1 of 3 cancer cells; grade 1b, marked changes in ≥ 1 of 3 but < 2 of 3 cancer cells; grade 2, marked changes in ≥ 2 of 3 cancer cells; and grade 3, necrosis or disappearance of all cancer cells and replacement of all cancer cells by granuloma-like and/or fibrous tissue. The histopathologic response was defined as the proportion of patients whose tumors were classified as grade 1b, 2, or 3.^{23,24}

Post hoc subset analyses were used to determine correlations between the baseline Ki-67 index ($\geq 20\%$ vs $< 20\%$) and the best overall tumor response. The percentage change in the Ki-67 index for responders (patients whose best overall tumor response was a complete or partial response) versus nonresponders (patients whose best overall tumor response was stable or progressive disease) also was compared. Correlations between the baseline Ki-67 index and the histopathologic response at week 24 also were evaluated, and we used post hoc analyses to investigate correlations between changes in the Ki-67 index from baseline to week 24 and ER or PgR status at baseline. Positive ER and PgR status (Allred score ≥ 3) also was assessed at baseline and at week 24. Preoperative Endocrine Prognostic Index (PEPI) scores, which were calculated post hoc as the sum of risk points weighted by the size of the hazard ratio for tumor size, pathologic lymph node status, ER status, and Ki-67 expression for both recurrence-free and breast cancer-specific survival, were determined for each patient at surgery according to the methods described by Ellis and colleagues.²⁵

Statistical Analysis

The sample size calculation and the main statistical analyses have been described previously.²⁰ All randomized patients were included in the intent-to-treat analysis set.

In a post hoc exploratory analysis, chi-square tests were performed to compare the best overall tumor response at week 24 between baseline Ki-67 index categories ($\geq 20\%$ vs $< 20\%$) within each treatment group and between treatment groups within each baseline Ki-67 index category. A chi-square test also was used to compare the histopathologic response at 24 weeks between the baseline Ki-67 index categories within each treatment group. All tests were made at the nominal 2-sided significance level of .05.

RESULTS

Patients

In total, 197 patients were randomized to receive either anastrozole plus goserelin ($n = 98$) or tamoxifen plus goserelin ($n = 99$) (Fig. 1). Patient demographics and

TABLE 1. Patient Demographics and Baseline Tumor Characteristics

Characteristic	No. of Patients (%)	
	Anastrozole Plus Goserelin	Tamoxifen Plus Goserelin
No. of patients	98	99
Age: Median [range]	44 [28-54]	44 [30-53]
Body mass index: Mean \pm SD, kg/m ²	22.2 \pm 3.5	22.1 \pm 3.3
Histology type		
Infiltrating ductal carcinoma	87 (88.8)	91 (91.9)
Infiltrating lobular carcinoma	3 (3.1)	3 (3)
Other ^a	8 (8.2)	5 (5.1)
Tumor grade		
1	42 (42.9)	48 (48.5)
2	36 (36.7)	26 (26.3)
3	4 (4.1)	14 (14.1)
Not assessable	1 (1)	0 (0)
Not done	15 (15.3)	11 (11.1)
Hormone receptor status		
ER positive	98 (100)	99 (100)
PgR positive	93 (94.9)	87 (87.9)
HER2 negative	98 (100)	99 (100)

Abbreviations: ER, estrogen receptor; HER2, human epidermal growth factor receptor 2; PgR, progesterone receptor; SD, standard deviation.

^aOther included adenocarcinoma (n = 3).

baseline characteristics generally were well balanced between the treatment groups (Table 1). Paired samples for calculating changes in the Ki-67 index from baseline to week 24 were available for 89 patients in the anastrozole plus goserelin group and for 86 patients in the tamoxifen plus goserelin group.

Correlation of the Baseline Ki-67 Index and Best Overall Tumor Response

With a mean baseline Ki-67 index of 21.9% and 21.6% in the anastrozole and tamoxifen treatment groups, respectively, we used post hoc subset analyses to compare patients according to their baseline Ki-67 index (≥ 20 vs < 20 %). For anastrozole versus tamoxifen, best overall tumor response from baseline to week 24 was better with anastrozole plus goserelin versus tamoxifen plus goserelin both in patients who had a baseline Ki-67 index ≥ 20 % (73.2% vs 44.8%; $P = .002$) and in patients who had a baseline Ki-67 index < 20 % (52.5% vs 29%; $P = .035$) (Fig. 2A).

Within the treatment groups, the best overall tumor response from baseline to 24 weeks, as measured by MRI or CT, was significantly better with anastrozole plus goserelin for patients who had a baseline Ki-67 index ≥ 20 % than for those who had a baseline Ki-67 index < 20 % (73.2% vs 52.5%; $P = .036$). Among patients in the tamoxifen plus goserelin group, the best overall tumor response was 44.8% for patients who had a baseline Ki-67

index ≥ 20 % and 29% for those who had a baseline Ki-67 index < 20 % ($P = .118$) (Fig. 2A).

Correlation of the Baseline Ki-67 Index and Histopathologic Response

There was no significant difference in the histopathologic response between patients who had a baseline Ki-67 index ≥ 20 % versus patients who had a baseline Ki-67 index < 20 % in either treatment group (Fig. 2B).

Correlation of Change in the Ki-67 Index and Responders/Nonresponders

A waterfall plot of changes in the Ki-67 index for individual patients, illustrated according to responders or nonresponders, is provided in Figure 3. There was no apparent relation between a change in Ki-67 expression from baseline to week 24 for responders and nonresponders in either treatment group.

Correlation of the Baseline Ki-67 Index and Estrogen Receptor or Progesterone Receptor Status

In both treatment groups, positive ER status, as determined by the Allred score, was observed in 100% of patients at baseline and at week 24, and > 90 % of patients in both treatment groups were ER rich (baseline Allred score, ≥ 7). Therefore, it was not possible to determine any potential relation between the baseline ER Allred score and the percentage change in Ki-67 expression from baseline to week 24 in either treatment group.

In the anastrozole plus goserelin group, 98.9% of patients were positive for PgR expression at baseline, and 34.4% were positive for PgR expression at week 24. The percentage of patients with positive PgR status was not altered from baseline (91.9%) to week 24 (89.5%) in the tamoxifen plus goserelin group (Fig. 4A). In both treatment groups, the mean decrease in the Ki-67 index was greater in patients who had a baseline PgR Allred score ≥ 7 (anastrozole group, -88.8 %; tamoxifen group, -67.6 %), compared with patients who had a baseline PgR Allred score < 7 (anastrozole group, -74.1 %; tamoxifen group, -32.8 %) (Fig. 4B).

Preoperative Endocrine Prognostic Index Score

In the anastrozole treatment group, 33.3% of patients had a PEPI score of 0 compared with 11.4% in the tamoxifen group. Fewer patients (21.4%) had a PEPI score ≥ 4 in the anastrozole group compared with patients in the tamoxifen group (36.7%; $P = .002$) (Table 2).

DISCUSSION

In this exploratory analysis, we investigated changes in Ki-67 expression among patients from the STAGE study, a

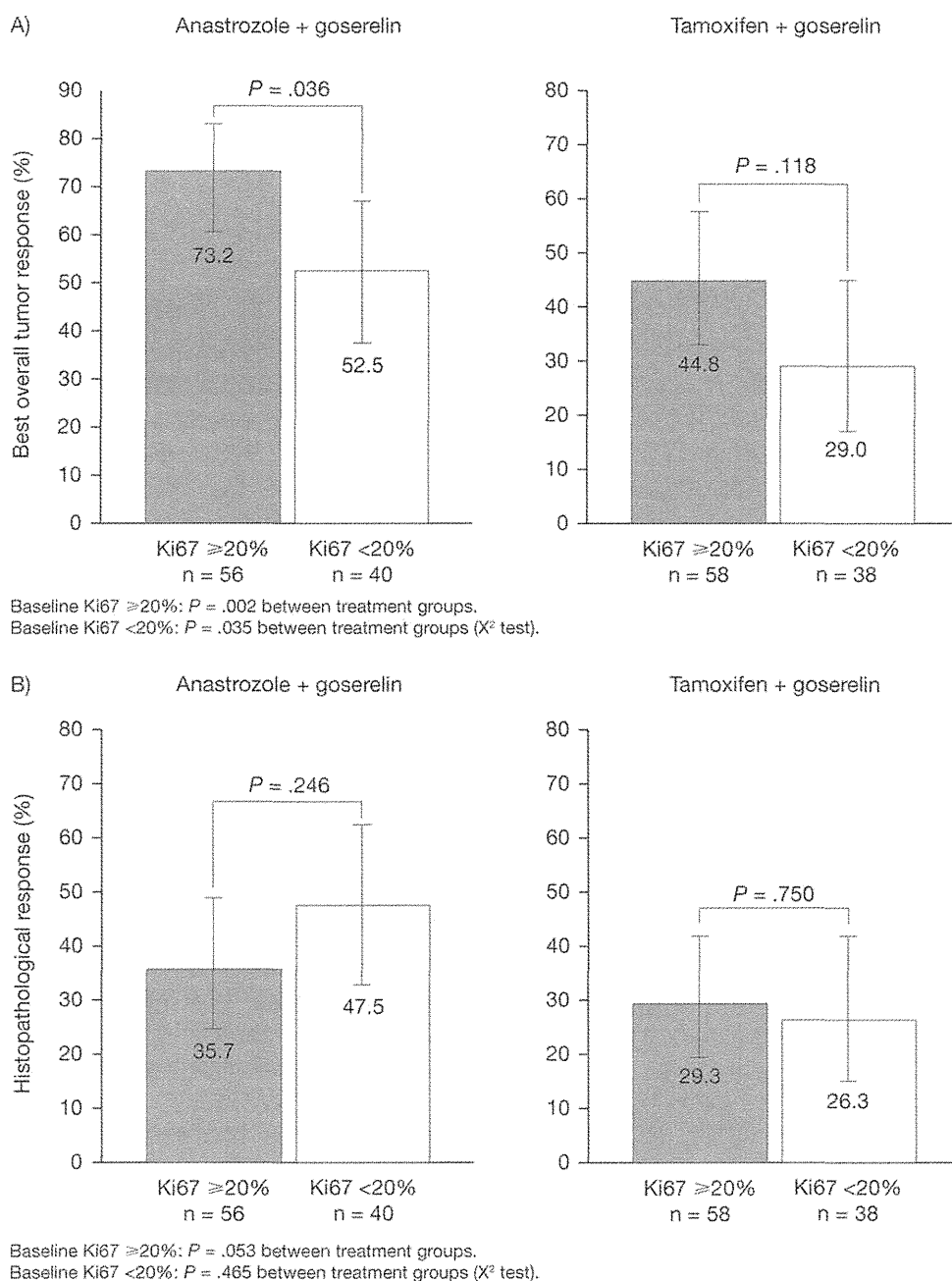


Figure 2. These charts illustrate the baseline Ki-67 index ($\geq 20\%$ vs $< 20\%$) according to (A) the best overall tumor response and (B) the histopathologic response at 24 weeks. Magnetic resonance imaging or computed tomography was used to measure responses. The best tumor response was defined a complete or partial response during the 24-week treatment period.

phase 3 randomized trial that compared tumor response for anastrozole plus goserelin versus response tamoxifen plus goserelin during 24 weeks of neoadjuvant treatment in premenopausal women with ER-positive breast cancer. The primary analysis indicated that the reduction in the Ki-67 index for patients who received goserelin was greater with anastrozole coadministration compared with tamoxifen, suggesting a greater inhibitory effect on tumor

cell proliferation with this treatment combination.²⁰ Given the reported clinical prognostic value of Ki-67 expression after short-term neoadjuvant endocrine therapy for breast cancer,¹⁹ this is in concordance with our finding that anastrozole combined with goserelin demonstrates a superior best overall tumor response compared with tamoxifen plus goserelin. Although Ki-67 is perceived as a reliable predictive endpoint, the outcomes of

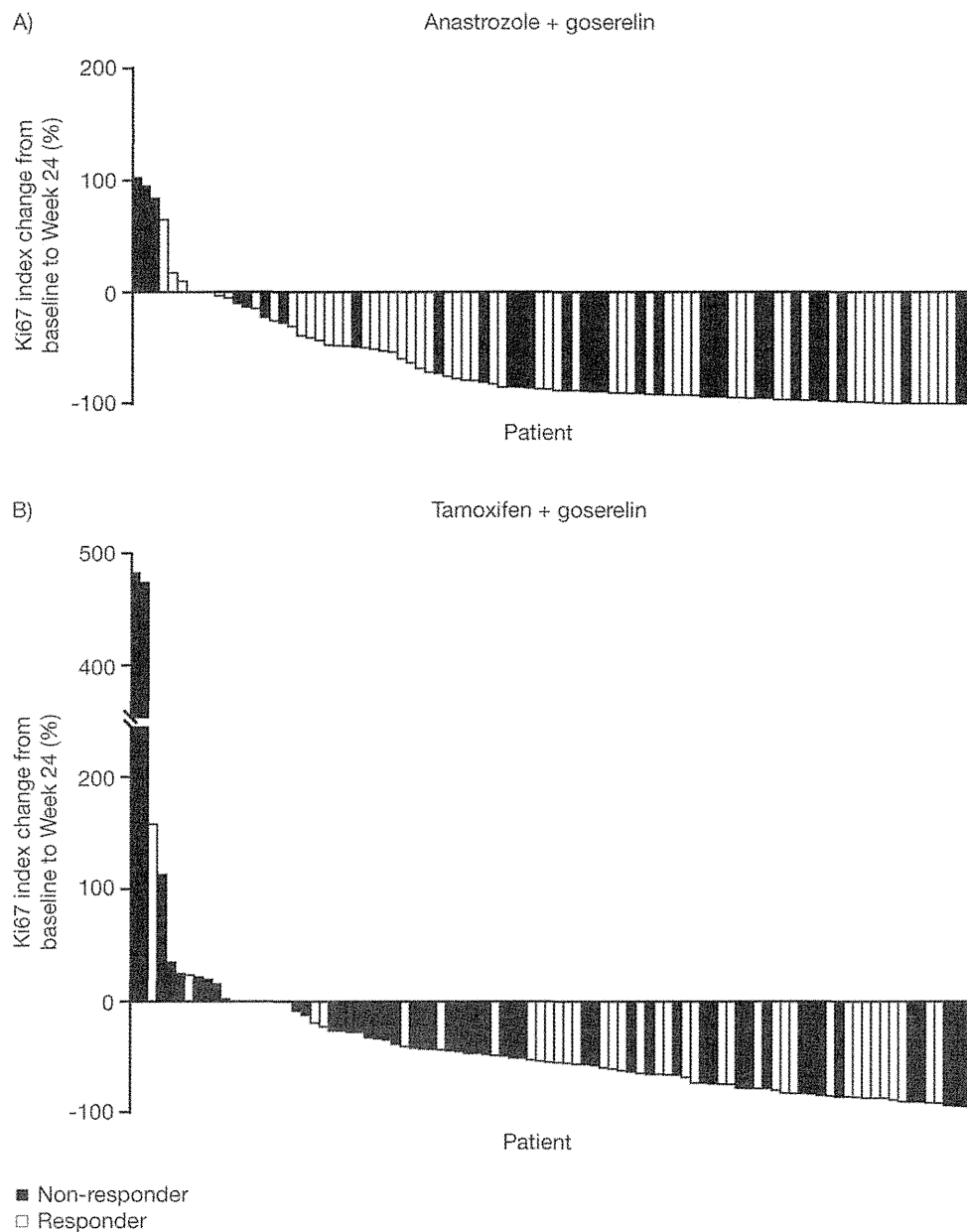


Figure 3. This is a waterfall plot of reductions in nuclear antigen Ki-67 levels in (A) the anastrozole plus goserelin treatment group and (B) the tamoxifen plus goserelin treatment group. Magnetic resonance imaging or computed tomography was used to measure responses. Responders were defined as those patients who had a complete or partial response during the 24-week treatment period.

the parallel adjuvant trial by the Austrian Breast and Colorectal Cancer Study Group (ABCSCG) did not reflect outcomes related to the Ki-67 changes we observed: Results from the ABCSCG-12 study indicated that there was no difference in disease-free survival between patients who received anastrozole versus tamoxifen (hazard ratio, 1.08; 95% CI, 0.81-1.44; $P = .591$).²⁶ The reason for this difference is not clear, although there were differences in the baseline characteristics of patients in each study: the

STAGE study assessed a more hormone-dependent phenotype of tumor (ER-positive/HER2-negative in the STAGE study vs ER-positive/HER2-negative and ER-positive/HER2-positive in the ABCSCG-12 trial), and the proportion of women with a body mass index $>25 \text{ kg/m}^2$ was lower in the STAGE study (17% vs 33%). The ABCSCG-12 group did not assess Ki-67 levels. It is also interesting to note that, as recently pointed out by Gonçalves et al,²⁷ in our study, serum estradiol suppression

recurrence) compared with the tamoxifen treatment group. The PEPI model has been validated previously and has indicated significant differences in recurrence-free survival in the adjuvant setting between 3 PEPI risk groups (PEPI risk scores of 0, 1-3, and ≥ 4), with a PEPI score of 0 indicating a very low risk of relapse.²⁵ Data from the adjuvant treatment setting will provide added knowledge for the individualization of future adjuvant treatments after neoadjuvant therapy for breast cancer.

Currently, very little is known about the prognostic effect of Ki-67 in premenopausal women. However, in 1 recent study, the prognostic significance of Ki-67 was investigated in women with ER-positive breast cancer who had received short-term presurgical tamoxifen, and Decensi and colleagues reported that the Ki-67 response was a good predictor of recurrence-free survival and overall survival.³³

To our knowledge, this is the first randomized study to investigate the potential of Ki-67 as a clinical biomarker for AI efficacy in premenopausal women with ER-positive breast cancer. It has been demonstrated that a reduction in Ki-67 expression as a result of neoadjuvant AI treatment can be a potentially useful marker of improved surgical outcomes in postmenopausal women with ER-positive breast cancer, and such a reduction has been identified as predictive of favorable outcomes in the adjuvant treatment period.³⁴ A reduction in Ki-67 expression during neoadjuvant treatment reportedly was greater with anastrozole versus tamoxifen in postmenopausal women who had ER-positive breast cancer,¹⁸ and a parallel result also was observed in the corresponding adjuvant trial, in which recurrence-free survival also was greater for those who received anastrozole.⁸ Yet another similar result was observed for letrozole, in which a greater Ki-67 reduction was observed compared with tamoxifen in the neoadjuvant setting.³⁵ Greater clinical effectiveness also was observed for letrozole in the neoadjuvant setting, both in terms of the objective response rate and the rate of breast-conserving surgery.³⁶

In conclusion, tumor response was greater with anastrozole compared with tamoxifen, regardless of the baseline Ki-67 index, in premenopausal women who received goserelin as neoadjuvant therapy for ER-positive, early stage breast cancer. The current results indicate that endocrine therapy may offer a more tolerable treatment option than cytotoxic chemotherapy as neoadjuvant treatment for these patients, and further studies of the anastrozole plus goserelin treatment combination in this setting are warranted.

FUNDING SOURCES

This work was supported by AstraZeneca.

CONFLICT OF INTEREST DISCLOSURES

Dr. Iwase has received honoraria from AstraZeneca and research funding from AstraZeneca; Chugai Pharmaceutical Company, Ltd.; Novartis; and Takeda. Mr. Hayashi is an employee and holds stock ownership with AstraZeneca. Dr. Noguchi has received honoraria and research funding from and has acted in a consultant or in an advisory role for AstraZeneca.

REFERENCES

1. Goldhirsch A, Ingle JN, Gelber RD, Coates AS, Thurlimann B, Senn H-J. Thresholds for therapies: highlights of the St Gallen International Expert Consensus on the primary therapy of early breast cancer 2009. *Ann Oncol*. 2009;20:1319-1329.
2. Jonat W, Kaufmann M, Blamey RW, et al. A randomised study to compare the effect of the luteinising hormone releasing hormone (LHRH) analogue goserelin with or without tamoxifen in pre- and perimenopausal patients with advanced breast cancer. *Eur J Cancer*. 1995;31A:137-142.
3. Jakesz R, Hausmaninger H, Kubista E, et al. Randomized adjuvant trial of tamoxifen and goserelin versus cyclophosphamide, methotrexate, and fluorouracil: evidence for the superiority of treatment with endocrine blockade in premenopausal patients with hormone-responsive breast cancer—Austrian Breast and Colorectal Cancer Study Group Trial 5. *J Clin Oncol*. 2002;20:4621-4627.
4. Mouridsen H, Gershonovich M, Sun Y, et al. Superior efficacy of letrozole versus tamoxifen as first-line therapy for postmenopausal women with advanced breast cancer: results of a phase III study of the International Letrozole Breast Cancer Group. *J Clin Oncol*. 2001;19:2596-2606.
5. Nabholz JM, Buzdar A, Pollak M, et al. Anastrozole is superior to tamoxifen as first-line therapy for advanced breast cancer in postmenopausal women: results of a North American multicenter randomized trial. Arimidex Study Group. *J Clin Oncol*. 2000;18:3758-3767.
6. Bonnetterre J, Thurlimann B, Robertson JF, et al. Anastrozole versus tamoxifen as first-line therapy for advanced breast cancer in 668 postmenopausal women: results of the Tamoxifen or Arimidex Randomized Group Efficacy and Tolerability study. *J Clin Oncol*. 2000;18:3748-3757.
7. Paridaens RJ, Dirix LY, Beex LV, et al. Phase III study comparing exemestane with tamoxifen as first-line hormonal treatment of metastatic breast cancer in postmenopausal women: the European Organisation for Research and Treatment of Cancer Breast Cancer Cooperative Group. *J Clin Oncol*. 2008;26:4883-4890.
8. Baum M, Budzar AU, Cuzick J, et al. Anastrozole alone or in combination with tamoxifen versus tamoxifen alone for adjuvant treatment of postmenopausal women with early breast cancer: first results of the ATAC randomised trial. *Lancet*. 2002;359:2131-2139.
9. Howell A, Cuzick J, Baum M, et al. Results of the ATAC (Arimidex, Tamoxifen, Alone or in Combination) trial after completion of 5 years' adjuvant treatment for breast cancer. *Lancet*. 2005;365:60-62.
10. Dowsett M, Cuzick J, Ingle J, et al. Meta-analysis of breast cancer outcomes in adjuvant trials of aromatase inhibitors versus tamoxifen. *J Clin Oncol*. 2010;28:509-518.
11. Cuzick J, Sestak I, Baum M, et al. Effect of anastrozole and tamoxifen as adjuvant treatment for early-stage breast cancer: 10-year analysis of the ATAC trial. *Lancet Oncol*. 2010;11:1135-1141.
12. van de Velde CJ, Rea D, Seynaeve C, et al. Adjuvant tamoxifen and exemestane in early breast cancer (TEAM): a randomised phase 3 trial. *Lancet*. 2011;377:321-331.
13. Forward DP, Cheung KL, Jackson L, Robertson JF. Clinical and endocrine data for goserelin plus anastrozole as second-line endocrine therapy for premenopausal advanced breast cancer. *Br J Cancer*. 2004;90:590-594.
14. Gnant M, Mlineritsch B, Schippinger W, et al. Endocrine therapy plus zoledronic acid in premenopausal breast cancer. *N Engl J Med*. 2009;360:679-691.

15. Tan MC, Al Mushawah F, Gao F, et al. Predictors of complete pathological response after neoadjuvant systemic therapy for breast cancer. *Am J Surg*. 2009;198:520-525.
16. Semiglazov VF, Semiglazov VV, Dashyan GA, et al. Phase 2 randomized trial of primary endocrine therapy versus chemotherapy in postmenopausal patients with estrogen receptor-positive breast cancer. *Cancer*. 2007;110:244-254.
17. Weigel MT, Dowsett M. Current and emerging biomarkers in breast cancer: prognosis and prediction. *Endocr Relat Cancer*. 2010;17:R245-R262.
18. Dowsett M, Smith IE, Ebbs SR, et al. Short-term changes in Ki-67 during neoadjuvant treatment of primary breast cancer with anastrozole or tamoxifen alone or combined correlate with recurrence-free survival. *Clin Cancer Res*. 2005;11:951s-958s.
19. Dowsett M, Smith IE, Ebbs SR, et al. Prognostic value of Ki-67 expression after short-term presurgical endocrine therapy for primary breast cancer. *J Natl Cancer Inst*. 2007;99:167-170.
20. Masuda N, Sagara Y, Kinoshita T, et al. Neoadjuvant anastrozole versus tamoxifen in patients receiving goserelin for premenopausal breast cancer (STAGE): a double-blind, randomised phase 3 trial. *Lancet Oncol*. 2012;13:345-352.
21. Therasse P, Arbuck SG, Eisenhauer EA, et al. New guidelines to evaluate the response to treatment in solid tumors. European Organization for Research and Treatment of Cancer, National Cancer Institute of the United States, National Cancer Institute of Canada. *J Natl Cancer Inst*. 2000;92:205-216.
22. Allred DC, Harvey JM, Berardo M, Clark GM. Prognostic and predictive factors in breast cancer by immunohistochemical analysis. *Mod Pathol*. 1998;11:155-168.
23. Sakamoto G, Inaji H, Akiyama F, et al. General rules for clinical and pathological recording of breast cancer 2005. *Breast Cancer*. 2005;12(suppl):S1-S27.
24. Kurosumi M, Takatsuka Y, Watanabe T, et al. Histopathological assessment of anastrozole and tamoxifen as preoperative (neoadjuvant) treatment in postmenopausal Japanese women with hormone receptor-positive breast cancer in the PROACT trial. *J Cancer Res Clin Oncol*. 2008;134:715-722.
25. Ellis MJ, Tao Y, Luo J, et al. Outcome prediction for estrogen receptor-positive breast cancer based on postneoadjuvant endocrine therapy tumor characteristics. *J Natl Cancer Inst*. 2008;100:1380-1388.
26. Gnant M, Mlineritsch B, Stoeger H, et al. Adjuvant endocrine therapy plus zoledronic acid in premenopausal women with early-stage breast cancer: 62-month follow-up from the ABCSG-12 randomised trial. *Lancet Oncol*. 2011;12:631-641.
27. Goncalves R, Ma C, Luo J, Suman V, Ellis MJ. Use of neoadjuvant data to design adjuvant endocrine therapy trials for breast cancer. *Nat Rev Clin Oncol*. 2012;9:223-229.
28. Dowsett M, Smith IE, Ebbs SR, et al. Proliferation and apoptosis as markers of benefit in neoadjuvant endocrine therapy of breast cancer. *Clin Cancer Res*. 2006;12:1024s-1030s.
29. Endo Y, Toyama T, Takahashi S, et al. High estrogen receptor expression and low Ki-67 expression are associated with improved time to progression during first-line endocrine therapy with aromatase inhibitors in breast cancer. *Int J Clin Oncol*. 2011;16:512-518.
30. Toi M, Saji S, Masuda N, et al. Ki-67 index changes, pathological response and clinical benefits in primary breast cancer patients treated with 24 weeks of aromatase inhibition. *Cancer Sci*. 2011;102:858-865.
31. Urruticoechea A, Smith IE, Dowsett M. Proliferation marker Ki-67 in early breast cancer. *J Clin Oncol*. 2005;23:7212-7220.
32. Mlineritsch B, Tausch C, Singer C, et al. Exemestane as primary systemic treatment for hormone receptor positive post-menopausal breast cancer patients: a phase II trial of the Austrian Breast and Colorectal Cancer Study Group (ABCSG-17). *Breast Cancer Res Treat*. 2008;112:203-213.
33. Decensi A, Guerrieri-Gonzaga A, Gandini S, et al. Prognostic significance of Ki-67 labeling index after short-term presurgical tamoxifen in women with ER-positive breast cancer. *Ann Oncol*. 2011;22:582-587.
34. Ellis MJ, Suman VJ, Hoog J, et al. Randomized phase II neoadjuvant comparison between letrozole, anastrozole, and exemestane for postmenopausal women with estrogen receptor-rich stage 2 to 3 breast cancer: clinical and biomarker outcomes and predictive value of the baseline PAM50-based intrinsic subtype—ACOSOG Z1031. *J Clin Oncol*. 2011;29:2342-2349.
35. Ellis MJ, Ma C. Letrozole in the neoadjuvant setting: the P024 trial. *Breast Cancer Res Treat*. 2007;105(suppl 1):33-43.
36. Eiermann W, Paepke S, Appfelstaedt J, et al. Preoperative treatment of postmenopausal breast cancer patients with letrozole: a randomized double-blind multicenter study. *Ann Oncol*. 2001;12:1527-1532.

Integration of Cell Line and Clinical Trial Genome-Wide Analyses Supports a Polygenic Architecture of Paclitaxel-Induced Sensory Peripheral Neuropathy

Heather E. Wheeler¹, Eric R. Gamazon², Claudia Wing¹, Uchenna O. Njiaju¹, Chidiamara Njoku¹; Robert Michael Baldwin³, Kouros Owzar⁴, Chen Jiang⁴, Dorothy Watson⁴, Ivo Shterev⁴, Michiaki Kubo⁵, Hitoshi Zembutsu⁶, Eric P. Winer³, Clifford A. Hudis⁷, Lawrence N. Shulman⁸, Yusuke Nakamura^{1,5}, Mark J. Ratain¹, and Deanna L. Kroetz³ for the Cancer and Leukemia Group B; Nancy J. Cox², and Mary Eileen Dolan¹

Abstract

Purpose: We sought to show the relevance of a lymphoblastoid cell line (LCL) model in the discovery of clinically relevant genetic variants affecting chemotherapeutic response by comparing LCL genome wide association study (GWAS) results to clinical GWAS results.

Experimental Design: A GWAS of paclitaxel induced cytotoxicity was conducted in 247 LCLs from the HapMap Project and compared with a GWAS of sensory peripheral neuropathy in patients with breast cancer ($n = 855$) treated with paclitaxel in the Cancer and Leukemia Group B (CALGB) 40101 trial. Significant enrichment was assessed by permutation resampling analysis.

Results: We observed an enrichment of LCL cytotoxicity associated single nucleotide polymorphisms (SNP) in the sensory peripheral neuropathy associated SNPs from the clinical trial with concordant allelic directions of effect (empirical $P = 0.007$). Of the 24 SNPs that overlap between the clinical trial ($P < 0.05$) and the preclinical cytotoxicity study ($P < 0.001$), 19 of them are expression quantitative trait loci (eQTL), which is a significant enrichment of this functional class (empirical $P = 0.0447$). One of these eQTLs is located in *RFX2*, which encodes a member of the DNA binding regulatory factor X family. Decreased expression of this gene by siRNA resulted in increased sensitivity of Neuroscreen 1 (NS 1; rat pheochromocytoma) cells to paclitaxel as measured by reduced neurite outgrowth and increased cytotoxicity, functionally validating the involvement of *RFX2* in nerve cell response to paclitaxel.

Conclusions: The enrichment results and functional example imply that cellular models of chemotherapeutic toxicity may capture components of the underlying polygenic architecture of related traits in patients. *Clin Cancer Res*; 19(2); 491-9. ©2012 AACR.

Introduction

Paclitaxel is a tubulin targeting agent, widely used in the treatment of malignant disease, including ovarian, breast, lung, and head and neck cancers. Its long term use is often limited by sensory peripheral neuropathy, although the

mechanism of this toxicity is poorly understood. In one recent large study of more than 1,500 patients with breast cancer, severe (grade 3) sensory peripheral neuropathy occurred in 4% of patients treated with 4 cycles and 10% of patients treated with 6 cycles of single agent paclitaxel (1). Currently, genetic prediction of which patients with cancer may experience severe side effects induced by paclitaxel treatment is not possible (2), but several preliminary genetic associations have been made (3-8). If patients likely to experience such toxicities could be identified before beginning a paclitaxel regimen, patient care might be improved by implementing a reduced dose or an alternative treatment.

Because accruing large patient cohorts receiving the same drug regimen for discovery genome wide and replication studies in oncology is challenging, several groups of investigators have used lymphoblastoid cell lines (LCL) as a discovery tool and for follow up functional studies (9-13). LCLs are easy to experimentally manipulate and the genetic background and expression environment is known. The LCL model also permits functional validation studies of

Authors' Affiliations: Sections of ¹Hematology/Oncology and ²Genetic Medicine, Department of Medicine, University of Chicago, Chicago, Illinois; ³Department of Bioengineering and Therapeutic Sciences, School of Pharmacy and Medicine, University of California, San Francisco, San Francisco, California; ⁴Department of Biostatistics and Bioinformatics, Duke University, Durham, North Carolina; ⁵Center for Genomic Medicine, RIKEN, Yokohama, Japan; ⁶Dana Farber Cancer Institute, Boston, Massachusetts; and ⁷Memorial Sloan Kettering Cancer Center, New York

Note: Supplementary data for this article are available at Clinical Cancer Research Online (<http://clincancerres.aacrjournals.org/>).

Corresponding Author: Mary Eileen Dolan, Section of Hematology/Oncology, Department of Medicine, University of Chicago, 900 E. 57th St., Chicago, IL 60637. Phone: 773 702 4441; E mail: edolan@medicine.bsd.uchicago.edu

doi: 10.1158/1078-0432.CCR.12.2618

©2012 American Association for Cancer Research.

Translational Relevance

Lymphoblastoid cell lines (LCL) have been used in chemotherapeutic pharmacogenomic marker discovery due to their ease of experimental manipulation, extensive genotype catalogs, and lack of the *in vivo* confounders present in clinical samples. One important question is how well these cell based models generate clinically relevant single nucleotide polymorphisms (SNP) associated with patient toxicity. We compared genome wide association study (GWAS) results of paclitaxel induced cytotoxicity in LCLs and paclitaxel induced peripheral neuropathy in patients with breast cancer. We observed significant overlap between the clinical and LCL studies, thus confirming a role for the LCL model in the analysis of at least a subset of genes involved in patient paclitaxel response. One overlap gene, *RFX2*, was functionally validated in a nerve cell model of paclitaxel response. Peripheral neuropathy is an often dose limiting toxicity induced by paclitaxel treatment. If physicians could predict which patients are more likely to experience this severe toxicity, lower doses or alternative treatments could be prescribed.

candidate markers and genes discovered in both preclinical and clinical studies (14, 15). However, a critical question is how well this cell based model generates clinically relevant markers and genes associated with patient response to drug. Recently, a few chemotherapeutic response single nucleotide polymorphisms (SNP) discovered in LCLs have been replicated in patient populations by associating with phenotypes such as tumor response and overall survival in patients receiving the same drug (16–19); however, these studies tested the individual variants most associated with the LCL phenotypes. We sought to understand to what extent the overall genetic architecture of patient response to chemotherapy can be captured by LCLs by investigating beyond just the top few signals. In contrast to previous studies that tested single SNPs, we use an enrichment method (20) to determine in a systematic manner whether top genome wide association study (GWAS) SNPs for paclitaxel induced sensory peripheral neuropathy in patients with breast cancer (3) are more likely to also be paclitaxel induced cytotoxicity SNPs identified in LCLs than expected by chance.

In this study, we found that SNPs associated with patient paclitaxel induced neuropathy are enriched for SNPs associated with paclitaxel induced cytotoxicity in HapMap LCLs. This significant enrichment confirms that LCLs are a useful model in the study of a subset of shared genes involved in patient toxicity. The overlap SNPs are predominantly expression quantitative trait loci (eQTL) as defined previously (21), therefore supporting an enriched functional role for these significant SNPs. We show a functional role for one eQTL host gene (*RFX2*) in paclitaxel toxicity, using a cellular model of peripheral neuropathy. These results are

consistent with the hypothesis that the cell based models capture components of the underlying genetic architecture for paclitaxel induced sensory peripheral neuropathy.

Materials and Methods

Cytotoxicity assays

HapMap LCLs from a population with Northern and Western European ancestry from Utah (HAPMAPPT01, CEU, $n = 77$), a Yoruba population in Ibadan, Nigeria (HAPMAPPT03, YRI, $n = 87$), and an African American population from the Southwest of the United States (HAPMAPPT07, ASW, $n = 83$) were treated with 12.5 nmol/L paclitaxel and cytotoxicity was determined using an AlamarBlue (Invitrogen) cellular growth inhibition assay as described (22). The cytotoxicity phenotype used in the LCL GWAS was mean percentage survival at 12.5 nmol/L paclitaxel determined from 6 replicates from 2 independent experiments. Percentage survival values for each cell line were \log_2 transformed before statistical analysis to form an approximately normal distribution in each population.

LCL genome wide meta analysis

A GWAS of paclitaxel induced cytotoxicity was conducted on each of the 3 populations separately. Greater than 2 million SNPs from HapMap r27 [minor allele frequency (MAF) > 0.05 within the panel, no Mendelian errors and in Hardy Weinberg equilibrium ($P > 0.001$)] were tested for association with paclitaxel cytotoxicity in each population, using the quantitative trait disequilibrium test total association model (23). To control for population structure in the admixed ASW population, local ancestry at each genotyped SNP locus was estimated using HAPMIX (24) and to increase genome coverage of the ASW, ungenotyped markers were imputed using BEAGLE (25) as previously described (26). Genomic control λ_{GC} values (27) were calculated for the GWAS of each population. Studies with λ_{GC} values greater than 1 were corrected for residual inflation of the test statistic by dividing the observed test statistic at each SNP by the λ_{GC} (27), and then the corresponding P values were carried through the meta analysis.

Using the software METAL, we combined SNP P values across the 3 population studies, taking into account a study specific weight (sample size) and direction of effect (positive or negative β ; ref. 28). This approach converted the direction of effect and P value observed in each study into a signed Z score, such that very negative Z scores indicate a small P value and an allele associated with higher drug sensitivity, whereas large positive Z scores indicate a small P value and an allele associated with higher drug resistance. Z scores for each SNP were combined across studies in a weighted sum, with weights proportional to the square root of the sample size for each study (28).

Patient samples and GWAS

Cancer and Leukemia Group B (CALGB) 40101 is a phase III trial comparing the efficacy of standard therapy cyclophosphamide and doxorubicin with single agent paclitaxel

as adjuvant therapy for breast cancer in women with 0 to 3 positive axillary lymph nodes. All study participants were enrolled in CALGB 40101 and gave their additional consent to participate in the pharmacogenetic companion study (CALGB 60202), which has been published (3). All patient research met state, federal, and Institutional Review Board guidelines. Germline DNA was isolated from 1,040 patients on the paclitaxel arm of CALGB 40101 and genotyped using the Illumina 610 Quad platform as described previously (3). Following quality control analysis, genotypes were available for 520,679 SNPs. Principal component (PC) analysis identified 855 genetic Europeans that were used in a GWAS of sensory peripheral neuropathy (3). A dose to event analysis was conducted, with an event defined as grade 2 or greater sensory peripheral neuropathy. The Cox score test, powered for additive genetic effects, was used to test these marginal associations. Only SNPs with MAFs more than 0.05 in the patient population and in Hardy Weinberg equilibrium in the CEU ($P > 0.001$) were used in the LCL GWAS comparisons.

Enrichment analysis

We conducted a permutation resampling analysis (29) to test for an enrichment of cytotoxicity associated SNPs (LCLs) among the paclitaxel induced sensory peripheral neuropathy associated SNPs (patients). To this end, the patient outcomes (cumulative dose and event indicator vectors) were randomly shuffled while keeping the genotype data fixed to preserve linkage disequilibrium. On the basis of this permutation replicate, the standardized Cox score statistics were recalculated for all the SNPs. This process was conducted 1,000 times. For each of the 1,000 permutation replicates, the number of SNPs that had $P < 0.05$ in the patient data, $P < 0.001$ in the LCL data, and the same direction of effect (the same allele associated with increased neuropathy and increased cytotoxicity) was calculated. The overlap distribution from the permutations was compared with the observed SNP overlap to generate an empirical P value, calculated as the proportion of permutations in which the number of LCL/patient overlap SNPs exceeds the observed number. To test the robustness of our findings, we calculated an empirical P value across a range of inclusion thresholds from $P < 0.001$ to $P < 0.1$. We also tested for enrichment of patient SNPs among the LCL SNPs by generating 1,000 randomized SNP sets the same size and MAF distribution as the observed LCL data at a range of P value thresholds to calculate empirical P values. In addition to the paclitaxel LCL cytotoxicity data, we compared the patient sensory peripheral neuropathy data with LCL cytotoxicity GWAS data from capecitabine (30) and carboplatin (13) as negative controls.

To test for eQTL enrichment in the LCL, patient, and LCL/patient overlap SNPs, we generated 10,000 randomized SNP sets each of the same size as the observed set of LCL cytotoxicity ($P < 0.001$), patient neuropathy ($P < 0.05$), or LCL/patient overlap SNPs. The randomized SNP sets were matched on MAF distribution of the observed list and sampled (without replacement) from the set of SNPs on

the Illumina 610 Quad platform, similar to the method of Gamazon and colleagues (31). We grouped the platform SNPs into discrete MAF bins of a width of 5%, from which the SNPs used in the simulations were selected. For each of the 10,000 sets, we determined the number of eQTLs ($P < 10^{-4}$) and calculated an empirical P value for enrichment. The eQTLs were defined previously and are available in the SCAN database (21, 31).

Filtering procedure for functional analysis

First, we determined which of the LCL/patient overlap SNPs from the enrichment analysis were located in or near (within 2 kb) gene transcripts (dbSNP build 129, human genome assembly build 36). Eleven of 24 overlap SNPs were in or near genes and genotyping intensity plots for these SNPs in the patient data are available in Supplementary Fig. S1. Second, we determined which SNPs within genes were also eQTLs (31) and prioritized by which had the most target genes ($P < 10^{-4}$). We also tested whether the expression of the eQTL target genes associated with paclitaxel induced cytotoxicity ($P < 0.05$) using previously published exon array data (32). A general linear model was constructed between gene expression and paclitaxel induced cytotoxicity with growth rate (33) and population as covariates. A Toeplitz covariance structure with 2 diagonal bands was used to allow for familial dependencies in the data as previously described (9).

siRNA

Neuroscreen 1 (NS 1) rat pheochromocytoma cells (Cellomics Inc.) were maintained in NS 1 media (RPMI supplemented with 10% horse serum, 5% fetal calf serum and 1% L-glutamine). Cells were seeded at a density of 1×10^5 cells/mL on collagen I coated plates and induced to differentiate by adding 20 ng/mL nerve growth factor (NGF, BD Biosciences) to the media 24 hours before transfection. Cells for cytotoxicity assays were plated in 96 well collagen I coated plates, whereas cells for expression quantification and neurite outgrowth assays were plated in 6 well collagen I coated plates. Pooled *Rfx2* siRNA (25 nmol/L; Qiagen; S101639659, S101639666, S101639673, and S101639680) or nontargeting control siRNA (Qiagen; 1027292) was transiently transfected into the NS 1 cells using DharmaFECT Reagent #1 (Dharmacon). Quantitative reverse transcription PCR (qRT-PCR) was conducted for *Rfx2* (Rn00501380 m1) and control gene *Gapdh* (4352338E) using TaqMan Gene Expression Assays (Applied Biosystems) 24 hours posttransfection in the neurite outgrowth assays and 24, 48, 72, and 96 hours posttransfection in the cytotoxicity assays to assess *Rfx2* knockdown in NS 1 cells. Expression of the potential *Rfx2* target genes *Cyp51* (Rn01526553 m1), *Bach1* (Rn01477344 m1), and *Cbara1* (Rn01644475 m1) was also measured by qRT-PCR at 24 hours post *siRfx2* transfection. Each qRT-PCR was run in duplicate and individual samples were run in triplicate on each plate. Percentage knockdown was calculated by dividing the relative *Rfx2* expression levels in the *siRfx2* sample by those in the nontargeting control sample.

Neurite outgrowth assays

Twenty four hours following siRNA transfection, transfection media was removed from the NS 1 cells and 0, 12.5, or 100 nmol/L paclitaxel in NS 1 media (supplemented with 20 ng/mL NGF) was added to either the *siRfx2* or nontargeting control cells. After 24 hours in the presence of paclitaxel, phase contrast images ($\times 10$) of the cells were taken using an Axiovert 200M inverted widefield fluorescence microscope (Zeiss). At least 500 cells per treatment in 6 randomly chosen fields were imaged and the longest neurite per cell was measured using ImageJ (34) software. The entire experiment was carried out in duplicate and mean neurite lengths were normalized relative to the 0 nmol/L drug treatment for each siRNA. Because tracing neurite lengths is somewhat qualitative, 2 scientists independently measured neurite lengths and the second scientist was blinded to siRNA/drug treatment. The mean of each set of measurements between the 2 scientists was assessed for significance by 2 way ANOVA (factors: siRNA treatment and drug treatment) to determine if the *siRfx2* affected neurite length upon paclitaxel treatment.

NS 1 cytotoxicity assays

Twenty four hours after siRNA transfection, transfection media was removed from the NS 1 cells and 0, 6.25, 12.5, 25, 50, or 100 nmol/L paclitaxel in NS 1 media (supplemented with 20 ng/mL NGF) in triplicate was added to either the *siRfx2* or nontargeting control cells. After 72 hours of paclitaxel treatment, ATP levels were measured using the CellTiter Glo assay (Promega) and percentage survival curves were generated. The entire experiment was done in duplicate and 2 way ANOVA was used to determine if the *siRfx2* significantly affected overall cytotoxicity upon paclitaxel treatment.

Results

Enrichment of LCL cytotoxicity SNPs in patient sensory peripheral neuropathy SNPs

We conducted a genome wide meta analysis (see Materials and Methods) to test common SNPs for association with paclitaxel induced cytotoxicity in LCLs. We compared the results from this analysis with those from clinical trial CALGB 40101, a GWAS of paclitaxel induced sensory peripheral neuropathy in patients with breast cancer (3). Neither study produced genome wide significant results ($\alpha < 0.05$) nor did the very top SNPs match between the 2 studies (Fig. 1). However, through a permutation resampling analysis of the CALGB patient data, we found that the top sensory peripheral neuropathy associated SNPs ($P < 0.05$) are significantly enriched for SNPs associated with paclitaxel induced cytotoxicity in LCLs ($P < 0.001$) with consistent allelic directions of effect (Fig. 2; empirical $P = 0.007$). The observed enrichment of 24 SNPs between the LCL and patient studies is likely paclitaxel specific, due to the sensory peripheral neuropathy SNPs not being enriched for either capecitabine or carboplatin induced cytotoxicity SNPs, which were tested as negative controls (Fig. 2). Positional information and effect sizes of all 24 overlap SNPs in the LCL and patient data can be found in Supplementary Table S1. When the inclusion thresholds for overlap SNPs were relaxed and when the LCL SNPs were tested for enrichment of patient SNPs, the significant overlap was present at a range of P value thresholds from 0.001 to 0.1, showing the robustness of our findings (Supplementary Table S2).

Enrichment of eQTLs in LCL/patient overlap SNPs

We tested the top paclitaxel induced LCL cytotoxicity SNPs ($P < 0.001$) and the top paclitaxel induced patient sensory peripheral neuropathy SNPs ($P < 0.05$) for eQTL

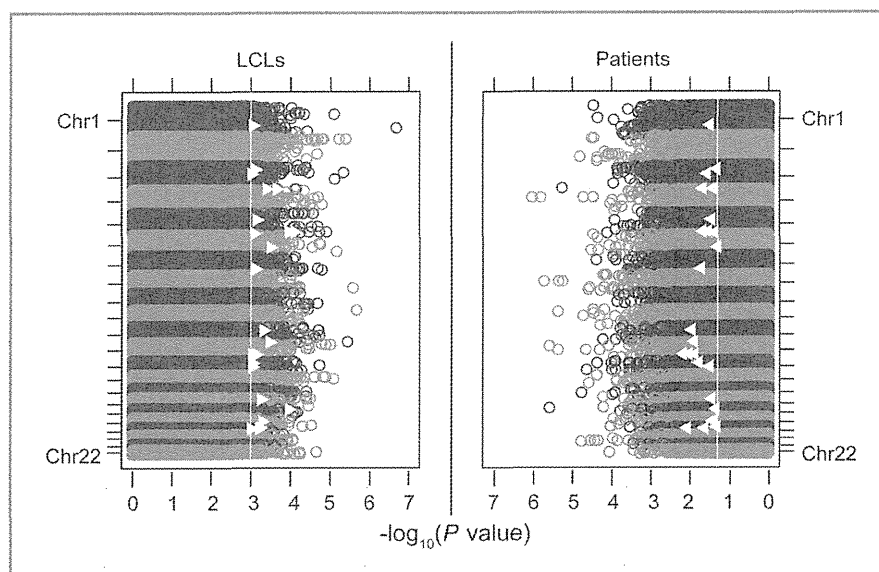


Figure 1. Comparison of individual GWAS results. Left, paclitaxel induced cytotoxicity in LCLs. Right, paclitaxel induced sensory peripheral neuropathy in patients. White lines represent the overlap thresholds used in the primary enrichment analysis ($P < 0.001$ for LCLs and $P < 0.05$ for patients) and white triangles represent the 24 overlap SNPs at these thresholds.

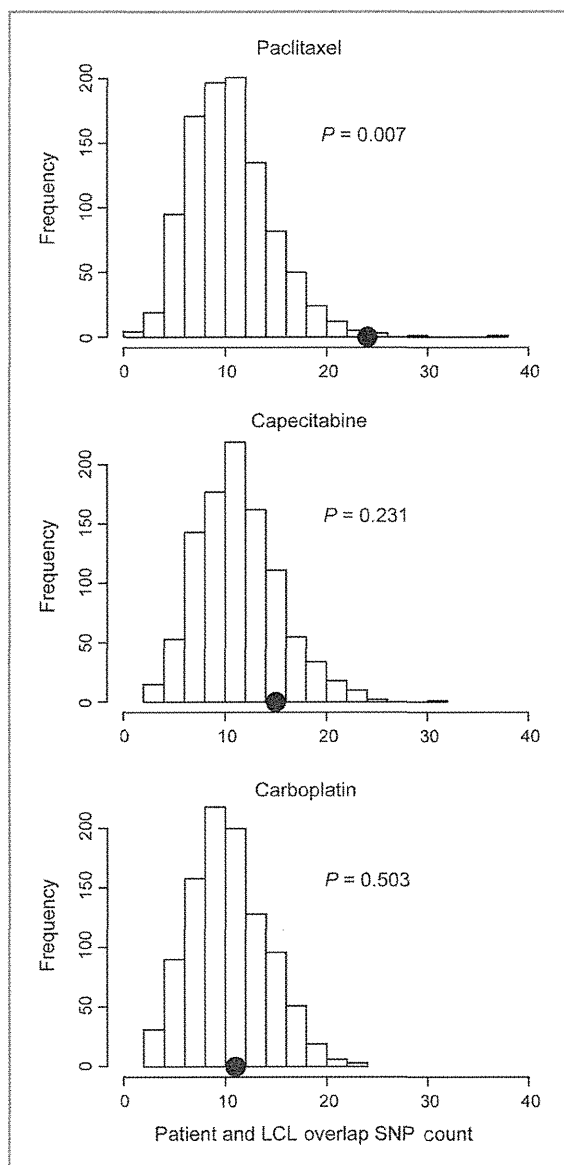


Figure 2. Patient paclitaxel induced sensory peripheral neuropathy SNPs are enriched for SNPs associated with paclitaxel induced cytotoxicity in LCLs. Distribution of chemotherapeutic induced cytotoxicity SNP ($P < 0.001$) count in 1,000 permutations of neuropathy phenotype genotype connections ($P < 0.05$). The dot is the observed SNP overlap at these thresholds. Of the 3 drug studies tested (paclitaxel, capecitabine, and carboplatin), only paclitaxel induced cytotoxicity SNPs were significantly enriched in the patient GWAS (empirical $P = 0.007$).

enrichment because these were the thresholds used in the primary overlap analysis. We compared the observed number of eQTLs at these thresholds to the number of eQTLs in 10,000 randomly selected MAF matched SNP sets (for details, see Materials and Methods). Neither cytotoxicity associated SNPs nor neuropathy associated SNPs alone were enriched for eQTLs (Fig. 3). However, we found that

the 24 paclitaxel LCL/patient overlap SNPs at these thresholds are enriched for eQTLs when compared with MAF matched SNP sets (empirical $P = 0.0447$), potentially revealing an important role for this functional class in paclitaxel toxicity.

Prioritization of LCL/patient overlap SNPs for functional analysis

First, we determined that 11 of 24 overlap SNPs from the enrichment analysis were located in or near (within 2 kb) gene transcripts (Table 1). The relationship of these 11 SNPs with paclitaxel induced sensory peripheral neuropathy in patients and LCL cytotoxicity is shown in Supplementary Fig. S2. Next, we determined which of these 11 SNPs within genes were also eQTLs (31). Of the 8 eQTLs, we determined which had the most potential target genes at an arbitrary threshold of $P < 10^{-4}$. The SNP in *RFX2* had 18 target genes, more than any other of the 8 eQTLs. In addition, we tested the expression of the target genes for association with paclitaxel induced cytotoxicity adjusted for growth rate (see Materials and Methods). We found that expression of 3 of the *RFX2* target genes associated with paclitaxel induced cytotoxicity (Table 1 and Supplementary Table S3); therefore, we pursued evaluating *RFX2* in a model of neuropathy.

Functional validation of *RFX2* in a paclitaxel induced peripheral neuropathy model

We used neuroscreen (NS 1) cells, a subclone of the rat pheochromocytoma cell line PC 12 that has previously been used as a research model for chemotherapy induced neuropathy (35, 36), to test *Rfx2*, the rat ortholog of *RFX2*, for functional involvement in paclitaxel response. Using siRNA, we decreased expression of *Rfx2* resulting in increased sensitivity of NS 1 cells to paclitaxel, as measured by reduced neurite outgrowth and increased cytotoxicity (Fig. 4). The 3 *RFX2* SNP target genes whose expression associated with paclitaxel induced cytotoxicity in LCLs are *CYP51A1*, *BACH1*, and *CBARA1* (Table 1; Fig. 5A C; $P < 0.05$). We measured the expression of these 3 potential *Rfx2* target genes upon knockdown of *Rfx2* in NS 1 cells and found that the expression of 1 of 3 genes, *Cyp51* (rat ortholog of *CYP51A1*), significantly decreased 24 hours posttransfection ($P < 0.05$), which is the expected direction of effect based on the LCL expression versus cytotoxicity data (Fig. 5D).

Discussion

We conducted a GWAS of paclitaxel induced cytotoxicity in LCLs and showed significant enrichment of the top cytotoxicity associated SNPs in a clinical GWAS of paclitaxel induced sensory peripheral neuropathy in patients with breast cancer. This robust enrichment shows that susceptibilities to increased cytotoxicity in LCLs and sensory peripheral neuropathy in patients with breast cancer likely have some genetic mechanisms in common and supports the role of LCLs as a preclinical model for paclitaxel toxicity studies. Furthermore, the top SNPs that overlap between the 2 studies were enriched for eQTLs. This eQTL enrichment

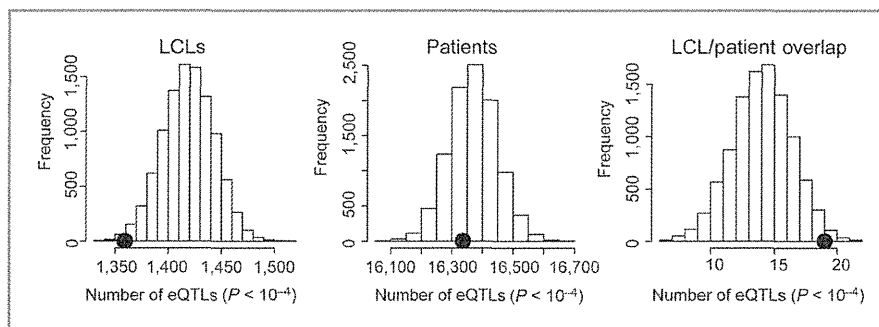


Figure 3. SNPs associated with both patient paclitaxel induced sensory peripheral neuropathy and LCL paclitaxel induced cytotoxicity are enriched for eQTLs. Distribution of eQTL ($P < 10^{-4}$) count in 10,000 simulations, each matching the MAF distribution of either LCL paclitaxel SNPs ($P < 0.001$), patient paclitaxel SNPs ($P < 0.05$), or the set of 24 LCL/patient overlap SNPs at these P value thresholds. Neither the LCL paclitaxel SNPs nor the patient paclitaxel SNPs alone were enriched for eQTLs, but the overlap SNP set between the 2 GWAS was enriched for eQTLs (empirical $P = 0.0447$).

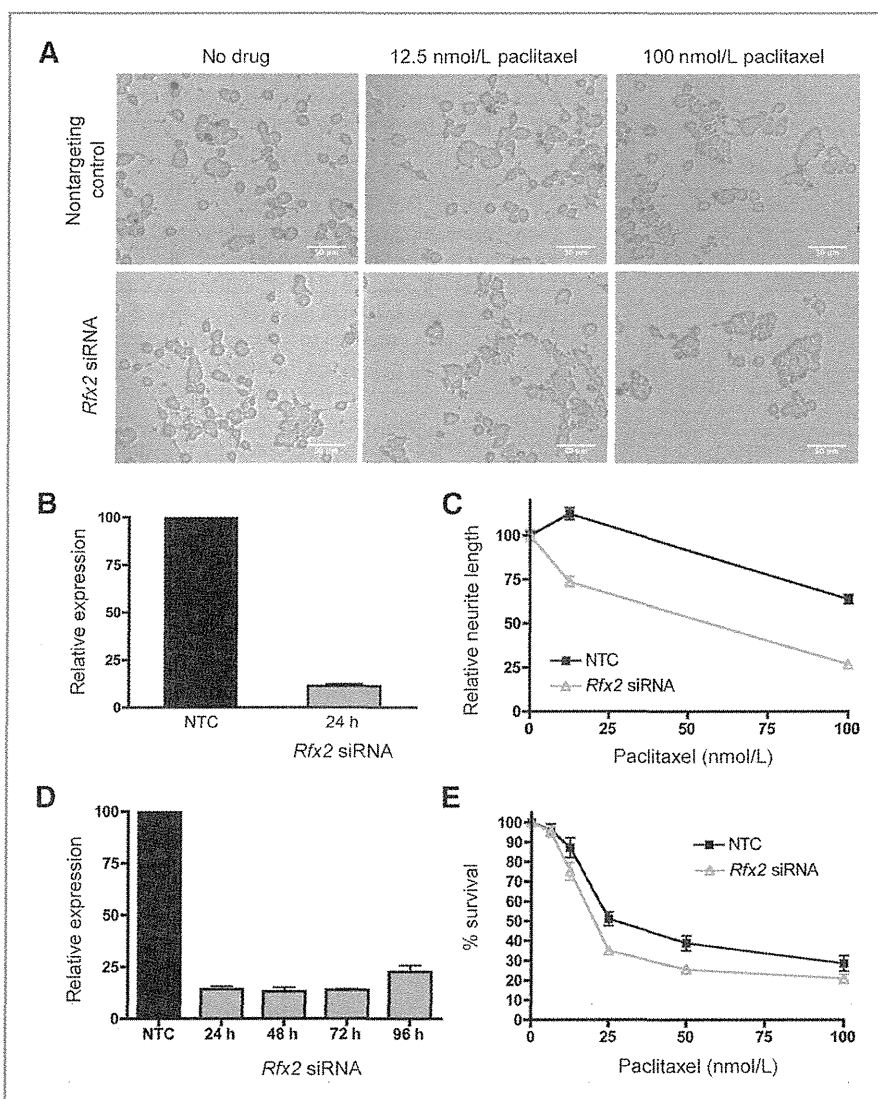


Figure 4. Functional validation of *RFX2* in paclitaxel response using a peripheral neuropathy cell model. A, representative micrographs comparing neurite lengths of NS 1 cells upon siRNA knockdown of *Rfx2* and treatment with paclitaxel ($\times 10$ phase contrast). B, relative gene expression 24 hours posttransfection in the 2 neurite length experiments. NTC, nontargeting control. C, decreased expression of *Rfx2* causes decreased neurite length of differentiating NS 1 cells ($P < 10^{-4}$) 24 hours post paclitaxel treatment (48 hours posttransfection). Error bars represent the SEM of the longest relative neurite length of at least 500 cells in each of 2 independent experiments. D, relative gene expression 24 to 96 hours posttransfection in the 2 cytotoxicity experiments. E, decreased expression of *Rfx2* causes decreased survival (increased cytotoxicity, $P < 10^{-4}$) of differentiating NS 1 cells measured by CellTiter Glo 72 hours post paclitaxel treatment (96 hours posttransfection). Error bars represent the SEM of survival in 2 independent experiments with 3 replicates each.

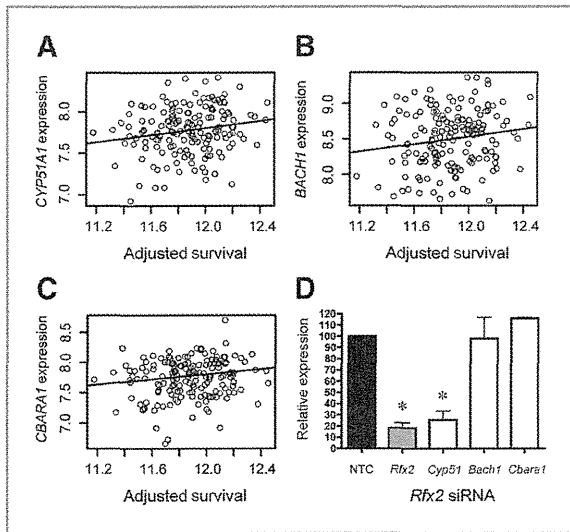


Figure 5. Target genes of *RFX2* eQTL rs7254081 in paclitaxel response. Increased baseline expression of the rs7254081 target genes (A) *CYP51A1*, (B) *BACH1*, and (C) *CBARA1* associate with increased cellular survival (adjusted for growth rate) of LCLs treated with 12.5 nmol/L paclitaxel ($P < 0.05$). D, *Rfx2* siRNA in NS 1 cells decreases the expression of *Rfx2* and *Cyp51*, but not *Bach1* and *Cbara1*, compared with the nontargeting control (NTC) 24 hours posttransfection. *, $P < 0.05$. Error bars represent the SEM of relative gene expression in 2 independent experiments with 3 replicates each.

indicates that SNPs associated with paclitaxel induced toxicity phenotypes may be functioning through gene regulatory mechanisms. Interestingly, neither GWAS alone was enriched for eQTLs. Thus, our integration method may be reducing noise and revealing important functional SNPs. An enrichment of eQTLs has previously been shown in SNPs associated with 6 other chemotherapeutic drugs,

which indicates that susceptibility to these drugs may depend on subtle gene expression differences across individuals (31).

The enrichment analyses were likely affected by the different linkage disequilibrium patterns among the populations studied. The LCL GWAS was a meta analysis of African, African American, and European populations, whereas the patient GWAS was conducted in Europeans. In the meta analysis, SNPs that are associated with cytotoxicity in all populations are prioritized over those associated in only one of the populations. We may have missed identifying European specific overlap alleles. However, because the population linkage disequilibrium patterns differ and because African populations have shorter linkage disequilibrium blocks, overlap SNPs are more likely to be functional SNPs rather than SNPs that simply tag a functional locus (37).

We functionally assessed the involvement of one overlap eQTL, *RFX2*, in the NS 1 neuropathy cell model. Paclitaxel has previously been shown to decrease neurite outgrowth in the parent clone of the NS 1 cell line (36). Here, we showed that decreased expression of *Rfx2* sensitizes NS 1 cells to paclitaxel by reducing neurite outgrowth and survival. This result validates our approach by showing that patient neuropathy and LCL cytotoxicity overlap analyses can reveal genes mechanistically involved in paclitaxel response. Although most previous work on *RFX2* in mammalian cells describes its role in spermatogenesis (38, 39), several studies point to a potential role for the protein in sensory neurons. *RFX2* and the related protein *RFX1* have been shown to directly bind and regulate the transcription of *ALMS1* (40). Mutations in *ALMS1* cause the rare genetic disorder Alström syndrome, which is characterized by neurosensory degeneration, metabolic defects, and cardiomyopathy (40). In addition, the regulatory factor X

Table 1. Paclitaxel-induced LCL cytotoxicity ($P < 0.001$) and paclitaxel-induced patient sensory peripheral neuropathy ($P < 0.05$) overlap SNPs located in genes

SNP	LCL cytotoxicity P value	Patient sensory peripheral neuropathy P value	Gene	eQTL	Number of target genes	Target genes associated with LCL paclitaxel induced cytotoxicity ^a ($P < 0.05$)
rs7254081	5.9E 04	4.8E 02	<i>RFX2</i>	yes	18	<i>CYP51A1</i> , <i>BACH1</i> , <i>CBARA1</i>
rs7642318	2.2E 04	3.9E 02	<i>TMEM44</i>	yes	6	
rs10933663	4.0E 04	2.1E 02	<i>TMEM44</i>	yes	4	
rs8002545	9.2E 04	3.1E 02	<i>DIS3</i>	yes	3	
rs4782010	5.5E 04	3.5E 02	<i>XYLT1</i>	yes	2	
rs11111539	7.9E 04	6.7E 03	<i>C12orf42</i>	yes	1	
rs7306825	7.2E 04	9.3E 03	<i>C12orf42</i>	yes	1	
rs8069856	1.1E 04	4.5E 02	<i>RICH2</i>	yes	1	
rs4868011	8.2E 04	4.2E 02	<i>KCNIP1</i>			
rs10778237	9.3E 04	1.3E 02	<i>C12orf42</i>			
rs323285	5.1E 04	3.7E 02	<i>KIAA1328</i>			

^aAdjusted for growth rate.

transcription factors present in *Caenorhabditis elegans* and *Drosophila*, which are called DAF 19 and RFX, respectively, regulate ciliated sensory neuron differentiation (41, 42).

Upon knockdown of *Rfx2* in NS 1 cells, the potential target gene *Cyp51* also decreased expression, which was the expected direction of effect based on the preliminary gene expression analysis in LCLs. However, *CYP51A1* does not contain an X box RFX binding domain (43) in the promoter region (2 kb upstream of the transcription start site), which means it is unlikely a direct target of *RFX2* and may instead be further downstream in the pathway. Alternatively, *RFX2* could be regulating an enhancer of *CYP51A1* that is further outside the gene region. *CYP51A1* is a member of the cytochrome P450 superfamily of enzymes, which catalyze many reactions involved in the metabolism of drugs and endogenous compounds. Specifically, *CYP51A1* is known to participate in the synthesis of cholesterol (44). *CYP51A1* has not been previously implicated in paclitaxel metabolism (45).

In the CALGB GWAS, one of the top SNPs that associated with patient paclitaxel induced sensory peripheral neuropathy (rs10771973, $P = 2.6 \times 10^{-6}$) is located in *FGD4* (3). Mutations in *FGD4* can cause the congenital peripheral neuropathy Charcot Marie Tooth disease type 4H, and thus the gene is a plausible candidate for involvement in variation in peripheral neuropathy induced by paclitaxel. This SNP association was replicated in a second cohort of self reported White patients with breast cancer ($n = 154$; $P = 0.013$) and in a cohort of self reported African American patients with breast cancer ($n = 117$; $P = 6.7 \times 10^{-3}$; ref. 3). However, this SNP was not associated with paclitaxel induced cytotoxicity in LCLs ($P = 0.65$). *FGD4* is not expressed in LCLs (21), and thus the SNP is not expected to function in this model system. While our integrative approach can reveal variants and genes acting in paclitaxel response in both patients and LCLs, it does not identify genes potentially acting in patients that are not expressed in LCLs.

Effectively, LCLs have been used as an additional cohort to study the pharmacogenomics of various chemotherapeutics (16–19) because limited resources and *in vivo* confounders make obtaining large, homogeneous patient cohorts difficult. Here, we saw greater SNP overlap than expected by chance between SNPs associated with paclitaxel induced cytotoxicity in LCLs and SNPs associated with paclitaxel induced sensory peripheral neuropathy in patients at multiple P value thresholds, which confirms a role for the LCL model in the analysis of at least a subset of genes involved in patient neurotoxicity. This significant enrichment among a relatively large number of top SNPs is consistent with an underlying polygenic architecture for paclitaxel induced

toxicity. Functional siRNA studies in the NS 1 neuropathy model validated the involvement of *RFX2* in paclitaxel toxicity, supporting our multi gene hypothesis. Our novel integrative enrichment approach that combines clinical and LCL GWAS results can be used to expand patient cohort sizes for any drug phenotype of interest, including other toxicities, such as neutropenia, to find genes of potential impact that can be studied in cellular models.

Disclosure of Potential Conflicts of Interest

E.P. Winer has a Commercial Research Grant from Roche. No potential conflicts of interest were disclosed by the other authors. The content of this article is solely the responsibility of the authors and does not necessarily represent the official views of the National Cancer Institute (NCI).

Authors' Contributions

Conception and design: H.E. Wheeler, E.R. Gamazon, K. Owzar, M. Kubo, C. Hudis, L.N. Shulman, Y. Nakamura, M.J. Ratain, N.J. Cox, M.E. Dolan
Development of methodology: H.E. Wheeler, E.R. Gamazon, C. Wing, K. Owzar, N.J. Cox

Acquisition of data (provided animals, acquired and managed patients, provided facilities, etc.): H.E. Wheeler, C. Wing, U.O. Njiaju, C. Njoku, R. M. Baldwin, M. Kubo, H. Zembutsu, C. Hudis, L.N. Shulman, Y. Nakamura, D.L. Kroetz, M.E. Dolan

Analysis and interpretation of data (e.g., statistical analysis, biostatistics, computational analysis): H.E. Wheeler, E.R. Gamazon, C. Wing, R. M. Baldwin, K. Owzar, D. Watson, I. Shterev, C. Hudis, L.N. Shulman, M.J. Ratain, D.L. Kroetz, N.J. Cox, M.E. Dolan

Writing, review, and/or revision of the manuscript: H.E. Wheeler, E.R. Gamazon, C. Wing, R.M. Baldwin, K. Owzar, C. Jiang, H. Zembutsu, E. Winer, C. Hudis, L.N. Shulman, M.J. Ratain, D.L. Kroetz, N.J. Cox, M.E. Dolan

Administrative, technical, or material support (i.e., reporting or organizing data, constructing databases): C. Wing, C. Hudis

Study supervision: H.E. Wheeler, C. Hudis, L.N. Shulman, M.E. Dolan

Acknowledgments

The authors thank the Pharmacogenomics of Anticancer Agents Research LCL core for maintaining and distributing LCLs.

Grant Support

This study is supported by NIH/NCI Cancer Biology Training grant T32CA009594 and National Research Service Award F32CA165823 (to H. E. Wheeler), NIH/National Institute of General Medical Sciences (NIGMS) Pharmacogenomics of Anticancer Agents grant U01GM61393 (to M.J. Ratain, N.J. Cox, M.E. Dolan, and K. Owzar), NIH/NIGMS Pharmacogenomics of Membrane Transporters grant U01GM61390 (to D.L. Kroetz), University of Chicago SPORE Grant NCI P50CA125183 (to M.E. Dolan), NIH/NCI Medical Oncology Training grant T32CA009566 (to U.O. Njiaju), and the Biobank Japan Project funded by the Japanese Ministry of Education, Culture, Sports, Science and Technology. This work is part of the NIH Pharmacogenomics Research Network-RIKEN Center for Genomic Medicine Global Alliance.

The research for CALGB 60202 and 40101 was supported, in part, by grants from the NCI (CA31946) to the CALGB (Monica M. Bertagnoli) and to the CALGB Statistical Center (Daniel J. Sargent, CA33601).

The costs of publication of this article were defrayed in part by the payment of page charges. This article must therefore be hereby marked *advertisement* in accordance with 18 U.S.C. Section 1734 solely to indicate this fact.

Received August 7, 2012; revised November 1, 2012; accepted November 8, 2012; published OnlineFirst November 30, 2012.

References

- Shulman LN, Cirincione CT, Berry DA, Becker HP, Perez EA, O'Regan R, et al. Six cycles of doxorubicin and cyclophosphamide or paclitaxel are not superior to four cycles as adjuvant chemotherapy for breast cancer in women with zero to three positive axillary nodes: cancer and leukemia group B 40101. *J Clin Oncol* 2012;30:4071–6.
- Pachman DR, Barton DL, Watson JC, Loprinzi CL. Chemotherapy induced peripheral neuropathy: prevention and treatment. *Clin Pharmacol Ther* 2011;90:377–87.
- Baldwin RM, Owzar K, Zembutsu H, Chhibber A, Kubo M, Jiang C, et al. A genome wide association study identifies novel loci for paclitaxel

- induced sensory peripheral neuropathy in CALGB 40101. *Clin Cancer Res* 2012;18:5099-109.
4. Green H, Soderkvist P, Rosenberg P, Horvath G, Peterson C. mdr 1 single nucleotide polymorphisms in ovarian cancer tissue: G2677T/A correlates with response to paclitaxel chemotherapy. *Clin Cancer Res* 2006;12:854-9.
 5. Hertz DL, Motsinger Reif AA, Drobish A, Winham SJ, McLeod HL, Carey LA, et al. CYP2C8*3 predicts benefit/risk profile in breast cancer patients receiving neoadjuvant paclitaxel. *Breast Cancer Res Treat* 2012;134:401-10.
 6. Leandro Garcia LJ, Leskela S, Jara C, Green H, Avall Lundqvist E, Wheeler HE, et al. Regulatory polymorphisms in beta tubulin IIa are associated with paclitaxel induced peripheral neuropathy. *Clin Cancer Res* 2012;18:4441-8.
 7. Leskela S, Leandro Garcia LJ, Mendiola M, Barriuso J, Inglada Perez L, Munoz I, et al. The miR 200 family controls beta tubulin III expression and is associated with paclitaxel based treatment response and progression free survival in ovarian cancer patients. *Endocr Relat Cancer* 2011;18:85-95.
 8. Sissung TM, Mross K, Steinberg SM, Behringer D, Figg WD, Sparre boom A, et al. Association of ABCB1 genotypes with paclitaxel mediated peripheral neuropathy and neutropenia. *Eur J Cancer* 2006;42:2893-6.
 9. Huang RS, Duan S, Bleibel WK, Kistner EO, Zhang W, Clark TA, et al. A genome wide approach to identify genetic variants that contribute to etoposide induced cytotoxicity. *Proc Natl Acad Sci U S A* 2007;104:9758-63.
 10. Li L, Fridley BL, Kalari K, Jenkins G, Batzler A, Weinshilboum RM, et al. Gemcitabine and arabinosylcytosin pharmacogenomics: genome wide association and drug response biomarkers. *PLoS ONE* 2009;4:e7765.
 11. Watters JW, Kraja A, Meucci MA, Province MA, McLeod HL. Genome wide discovery of loci influencing chemotherapy cytotoxicity. *Proc Natl Acad Sci U S A* 2004;101:11809-14.
 12. Wheeler HE, Dolan ME. Lymphoblastoid cell lines in pharmacogenomic discovery and clinical translation. *Pharmacogenomics* 2012;13:55-70.
 13. Wheeler HE, Gamazon ER, Stark AL, O'Donnell PH, Gorsic LK, Huang RS, et al. Genome wide meta analysis identifies variants associated with platinating agent susceptibility across populations. *Pharmacogenomics J*. 2011 Aug 16. [Epub ahead of print].
 14. Ingle JN, Schaid DJ, Goss PE, Liu M, Mushiroti T, Chapman JA, et al. Genome wide associations and functional genomic studies of musculoskeletal adverse events in women receiving aromatase inhibitors. *J Clin Oncol* 2010;28:4674-82.
 15. Shukla SJ, Duan S, Wu X, Badner JA, Kasza K, Dolan ME. Whole genome approach implicates CD44 in cellular resistance to carboplatin. *Hum Genomics* 2009;3:128-42.
 16. Huang RS, Johnatty SE, Gamazon ER, Im HK, Ziliak D, Duan S, et al. Platinum sensitivity related germline polymorphism discovered via a cell based approach and analysis of its association with outcome in ovarian cancer patients. *Clin Cancer Res* 2011;17:5490-500.
 17. Mitra AK, Crews K, Pounds S, Cao X, Downing JR, Raimondi S, et al. Impact of genetic variation in FKBP5 on clinical response in pediatric acute myeloid leukemia patients: a pilot study. *Leukemia* 2011;25:1354-6.
 18. Tan XL, Moyer AM, Fridley BL, Schaid DJ, Niu N, Batzler AJ, et al. Genetic variation predicting Cisplatin cytotoxicity associated with overall survival in lung cancer patients receiving platinum based chemotherapy. *Clin Cancer Res* 2011;17:5801-11.
 19. Ziliak D, O'Donnell PH, Im HK, Gamazon ER, Chen P, Delaney S, et al. Germline polymorphisms discovered via a cell based, genome wide approach predict platinum response in head and neck cancers. *Transl Res* 2011;157:265-72.
 20. Cox NJ, Gamazon ER, Wheeler HE, Dolan ME. Clinical translation of cell based pharmacogenomic discovery. *Clin Pharmacol Ther* 2012;92:425-7.
 21. Gamazon ER, Zhang W, Konkashbaev A, Duan S, Kistner EO, Nicolae DL, et al. SCAN: SNP and copy number annotation. *Bioinformatics* 2010;26:259-62.
 22. Nijaju UO, Gamazon ER, Gorsic LK, Delaney SM, Wheeler HE, Im HK, et al. Whole genome studies identify solute carrier transporters in cellular susceptibility to paclitaxel. *Pharmacogenet Genomics* 2012;22:498-507.
 23. Abecasis GR, Cookson WO, Cardon LR. Pedigree tests of transmission disequilibrium. *Eur J Hum Genet* 2000;8:545-51.
 24. Price AL, Tandon A, Patterson N, Barnes KC, Rafaels N, Ruczinski I, et al. Sensitive detection of chromosomal segments of distinct ancestry in admixed populations. *PLoS Genet* 2009;5:e1000519.
 25. Browning BL, Browning SR. A unified approach to genotype imputation and haplotype phase inference for large data sets of trios and unrelated individuals. *Am J Hum Genet* 2009;84:210-23.
 26. Wheeler HE, Gorsic LK, Welsh M, Stark AL, Gamazon ER, Cox NJ, et al. Genome wide local ancestry approach identifies genes and variants associated with chemotherapeutic susceptibility in African Americans. *PLoS ONE* 2011;6:e21920.
 27. Devlin B, Roeder K. Genomic control for association studies. *Bioinformatics* 1999;55:997-1004.
 28. Willer CJ, Li Y, Abecasis GR. METAL: fast and efficient meta analysis of genomewide association scans. *Bioinformatics* 2010;26:2190-1.
 29. Shterev ID, Jung SH, George SL, Owzar K, permGPU: using graphics processing units in RNA microarray association studies. *BMC Bioinformatics* 2010;11:329.
 30. O'Donnell PH, Stark AL, Gamazon ER, Wheeler HE, McIlwee BE, Gorsic L, et al. Identification of novel germline polymorphisms governing capecitabine sensitivity. *Cancer* 2012;118:4063-73.
 31. Gamazon ER, Huang RS, Cox NJ, Dolan ME. Chemotherapeutic drug susceptibility associated SNPs are enriched in expression quantitative trait loci. *Proc Natl Acad Sci U S A* 2010;107:9287-92.
 32. Duan S, Huang RS, Zhang W, Bleibel WK, Roe CA, Clark TA, et al. Genetic architecture of transcript level variation in humans. *Am J Hum Genet* 2008;82:1101-13.
 33. Stark AL, Zhang W, Mi S, Duan S, O'Donnell PH, Huang RS, et al. Heritable and non genetic factors as variables of pharmacologic phenotypes in lymphoblastoid cell lines. *Pharmacogenomics J* 2010;10:505-12.
 34. Schneider CA, Rasband WS, Eliceiri KW. NIH Image to ImageJ: 25 years of image analysis. *Nat Methods* 2012;9:671-5.
 35. Geldof AA. Nerve growth factor dependent neurite outgrowth assay; a research model for chemotherapy induced neuropathy. *J Cancer Res Clin Oncol* 1995;121:657-60.
 36. Verstappen CC, Postma TJ, Geldof AA, Heimans JJ. Amifostine protects against chemotherapy induced neurotoxicity: an *in vitro* investigation. *Anticancer Res* 2004;24:2337-41.
 37. Teo YY, Small KS, Kwiatkowski DP. Methodological challenges of genome wide association analysis in Africa. *Nat Rev Genet* 2010;11:149-60.
 38. Horvath GC, Kistler WS, Kistler MK. RFX2 is a potential transcriptional regulatory factor for histone H1t and other genes expressed during the meiotic phase of spermatogenesis. *Biol Reprod* 2004;71:1551-9.
 39. Wolfe SA, Wilkerson DC, Prado S, Grimes SR. Regulatory factor X2 (RFX2) binds to the H1t/TE1 promoter element and activates transcription of the testis specific histone H1t gene. *J Cell Biochem* 2004;91:375-83.
 40. Purvis TL, Hearn T, Spalluto C, Knorz VJ, Hanley KP, Sanchez Elsnert T, et al. Transcriptional regulation of the Alstrom syndrome gene ALMS1 by members of the RFX family and Sp1. *Gene* 2010;460:20-9.
 41. Swoboda P, Adler HT, Thomas JH. The RFX type transcription factor DAF 19 regulates sensory neuron cilium formation in *C. elegans*. *Mol Cell* 2000;5:411-21.
 42. Dubrulle R, Laurencon A, Vandaele C, Shishido E, Coulon Bubleux M, Swoboda P, et al. *Drosophila* regulatory factor X is necessary for ciliated sensory neuron differentiation. *Development* 2002;129:5487-98.
 43. Gajiwala KS, Chen H, Cornille F, Roques BP, Reith W, Mach B, et al. Structure of the winged helix protein hRFX1 reveals a new mode of DNA binding. *Nature* 2000;403:916-21.
 44. Halder SK, Fink M, Waterman MR, Rozman D. A cAMP responsive element binding site is essential for sterol regulation of the human lanosterol 14alpha demethylase gene (CYP51). *Mol Endocrinol* 2002;16:1853-63.
 45. Oshiro C, Marsh S, McLeod H, Carrillo M, Klein T, Altman R. Taxane Pathway. *Pharmacogenet Genomics* 2009;19:979-83.